# UC Berkeley
## UC Berkeley Electronic Theses and Dissertations

**Title**

The Role of Spontaneous Activity in the Development of Retinal Direction Selectivity

**Permalink**

https://escholarship.org/uc/item/39v0747k

**Author**

Hamby, Aaron Michael

**Publication Date**

2013

Peer reviewed|Thesis/dissertation

The Role of Spontaneous Activity in the Development of Retinal Direction Selectivity

By

Aaron Michael Hamby

A dissertation submitted in partial satisfaction of the requirements for the degree of

Doctor of Philosophy

in

Molecular & Cell Biology

in the

Graduate Division

of the

University of California, Berkeley

Committee in charge:

Professor Marla B. Feller, Chair
Professor Mu-ming Poo
Professor Ehud Y. Isacoff
Professor Mark A. Tanouye

Fall 2013

ABSTRACT


The Role of Spontaneous Retinal Activity in the Development of Direction Selectivity


By


Aaron Michael Hamby


Doctor of Philosophy in Molecular & Cell Biology

University of California, Berkeley

Professor Marla B. Feller, Chair

One of the most fascinating and distinctive features of the nervous system is that a vast number of neuronal cell-types arise from a limited number of precursors to assume a multitude of unique morphological and functional units throughout the brain. Furthermore, this mass of unique cell-types wire together with exquisite precision to form the neural circuits that do much of the work of the mature nervous system. How these highly specific and well-ordered assemblies of neurons achieve their ultimate structure and functional state is therefore one of the most important and challenging questions in modern neurobiology.

The direction selective circuit of the mammalian retina serves as a canonical example of how heterologous cell-types can be arranged in the nervous system to perform complex operations on sensory or synaptic input and transform noisy or mixed signals into specific channels that carry information about the outside world or internal states. How the specific synaptic connections underlying direction selectivity are specified, or how elements of the circuit acquire their unique identities is unclear. Both evoked and spontaneously generated neural activity have been well-documented to shape the assembly of neural circuits in diverse parts of the nervous system. Here, using a combination of multi-electrode array recordings, patch-clamp electrophysiology and anatomical and immunohistochemical techniques we test for a role of spontaneous activity in the development of retinal direction selectivity in mouse.

By developing transgenic mouse lines to identify direction selective ganglion cells for targeted investigation we identify a critical period of inhibitory synapse development crucial to the direction selective responses of these cells that occurs over the second post-natal week, a period dominated by glutamatergic retinal waves. Through the use of pharmacological and genetic manipulations to alter or block these retinal activity patterns we show that manipulations sufficient to disrupt the activity-dependent process of eye-specific segregation have no effect on

the emergence of robust direction selective responses, indistinguishable from age-matched wild type controls. These results indicate that spontaneous activity does not play a critical role in the development of the direction selective circuit in retina.

For my family,

And for all my teachers.

TABLE OF CONTENTS

LIST OF FIGURES

Chapter III:

ACKNOWLEDGEMENTS

Chapter 1, in full, is a reprint of the material as it appears in:

Aaron M. Hamby and Marla B. Feller. Development of direction selectivity, The New Visual Neurosciences, Nov 2013.

The dissertation author was the primary author of this chapter.

Chapter 2, in full, is a reprint of the material as it appears in:

Wei Wei, Aaron M. Hamby, Kaili Zhou, Marla B. Feller. Development of asymmetric inhibition underlying the development of direction selectivity in the retina, *Nature*, 2011 Jan 20;469(7330):402-6

The dissertation author was a coauthor of this paper. It is included with

permission from all authors.

Chapter 3 is original work in preparation. The dissertation author is the primary author.

VITA

1998-2003        B.S., Animal Physiology/ Neuroscience, Department of Biology
                 University of California, San Diego

2007-2013        Ph.D., Department of Molecular and Cell Biology
                 University of California, Berkeley

PUBLICATIONS

Hamby AM and Feller MB. Development of Direction Selectivity. The New Visual
        Neurosciences Nov 2013

Blankenship AG, Hamby AM, Firl A, Vyas S, Maxeiner S, Willecke K, Feller MB.
        The role of neuronal connexins 36 and 45 in shaping spontaneous firing patterns in the
        developing retina. Neurosci. 2011 Jul 6;31(27):9998-10008.

Wei W, Hamby AM, Zhou K, Feller MB: Development of asymmetric inhibition  underlying
        direction selectivity in the retina. Nature, 2011 Nature. 2011 Jan 20;469(7330):402-6.

AWARDS

2011-2013        Ruth L. Kirschstein National Research Service Award

# I. Development of Direction Selectivity

Motion constitutes one of the most salient cues for both vertebrate and invertebrate visual systems.  Indeed, multiple distinct circuits at various levels of the visual system are sensitive to the presence of moving objects. Perhaps, the best understood circuit that addresses the extraction of motion is that of the On-Off direction selective ganglion cell (DSGC) in the mammalian retina. DSGCs respond strongly to an image moving in the preferred direction and weakly to an image moving in the opposite, or null, direction. Though the cellular and synaptic bases of this computation are reasonably well understood, the wiring up of this circuit during development is mostly a mystery.  In this chapter, we describe how electrophysiological, imaging, genetic, and optogenetic techniques have allowed us to begin addressing questions regarding the development of direction selective circuits in the retina. This topic has also been the subject of several recent reviews (Borst & Euler, 2011; Elstrott & Feller, 2009; Wei & Feller, 2011).

## Overview of the direction selective circuit

Several distinct populations of DSGCs have been identified. Transgenic mice that label single subtypes of DSGCs with GFP indicate that the various subtypes (Figure 1b, and discussed below) may display intrinsic genetic differences.  However, we are far from a complete genetic description. Therefore, the present classification of DSGCs is based on their response properties, morphologies and target areas in the brain.

DSGCs fall into roughly three populations (reviewed in Berson, 2008; Borst & Euler, 2011; Vaney & Taylor, 2002; Wei & Feller, 2011):  1) On-Off DSGCs that project to the lateral geniculate nucleus and superior colliculus; 2) On-DSGCs that project to the medial terminal nucleus of the accessory optic system; and 3) Off-DSGCs cells that project to the superior colliculus.

On-Off DSGCs comprise four subtypes, each preferring motion along one of the cardinal directions: nasal, temporal, dorsal, or ventral (Figure 2A).  Each subtype forms an independent mosaic that tiles the retina with little intra-subtype dendritic overlap.  Thus, each point on the retina falls within the receptive fields of DSGCs that are sensitive to motion in all four cardinal directions.  Recently, Trenholm et al. (2011) described an On-Off DSGC with an asymmetric dendritic tree that points in the anterior direction. For this subtype, there is only a single preferred direction of motion, which lies parallel to the dendritic tree. This is in contrast to all other ON-OFF DSGC subtypes, which have more symmetric, and for which there is no correlation between patterns of dendritic arborization and directional preference. The projection pattern of this subtype is not yet known.

On-DSGCs comprise three subtypes, each preferring motion along one of the axes of rotation imposed by the extra-ocular muscles.  Each subtype of this DSGC class is also thought to form a mosaic, although these neurons are less populous than On-Off DSGCs and have larger dendritic trees (Rockhill, Daly, MacNeil, Brown, & Masland, 2002; W. Sun, Li, & He, 2002).  In

addition, On-DSGCs are more narrowly tuned to slower velocities (W. Sun, Deng, Levick, & He, 2006). Despite the different projection patterns and tuning properties, On-Off DSGCs and On-DSGCs share many circuit properties in the adult and appear to follow a similar developmental program, as described below.

Off-DSGCS comprise only one subtype and it prefers motion in the superior direction. These cells also tile the retina in a regular mosaic, and they are marked by an immunoglobin family protein, junctional adhesion molecule b (called JAM-b). The majority of JAM-b expressing neurons found in the central, nasal and temporal retina, roughly 85% of the entire population, have asymmetric dendritic trees that point down in retinal coordinates, parallel to the preferred direction. The remaining 15% are located in the ventral retina, have symmetric dendritic trees, and are not direction selective. Thus, the asymmetric structure of Off-DSGCs seems to play a role in generating their direction selectivity.

The direction selective circuit of On-Off DSGCs is schematized in Figure 1A. In brief, photoreceptors activate ON and OFF bipolar cells that provide excitatory glutamatergic input to the On and Off sublaminae of DSGCs. Bipolar cells also provide glutamatergic input to two mirror-symmetric populations of the GABAergic interneurons called starburst amacrine cells. One population of these amacrine cells has somas residing in the ganglion cell layer with processes costratifying with the On-sublamina processes of the On-Off DSGCs; the other population has somas residing in the inner-nuclear layer with processes co-stratifying with the OFF sublamina processes of these DSGCs.

The primary circuit model for generating direction selectivity in the retina states that stimulation in the null direction leads to stronger inhibition than stimulation in the preferred direction. Consistent with this hypothesis, paired recordings from starburst amacrine cells and DSGCs in mouse retina reveal that depolarization of a starburst amacrine cell on the null side induces significantly larger inhibitory currents in the DSGC than depolarization of this amacrine cell on the preferred side (Fried et al., 2002; Lee et al., 2010; Wei et al., 2011). These findings suggest that starburst amacrine cells create the asymmetric inhibitory fields that underlie direction selectivity in DSGCs via an asymmetric release of GABA that depends on the direction of motion of the light stimulus.

How does light moving in one direction lead to more GABA release than light moving in the other direction? A stimulus that leads to directional responses in DSGCs evokes symmetric responses from the starburst amacrine cells when measured at the level of soma depolarization. However, at the distal tips of these cells, two-photon calcium imaging reveals that calcium transients are larger for motion outward from the soma than for motion toward the soma (Euler, Detwiler, & Denk, 2002). Although this increase in intracellular calcium has not yet been shown to drive more GABA release, it has led to the hypothesis that the directionality of the starburst amacrine cell process underlies the asymmetric release of GABA.

Support for this hypothesis that directionality of a single starburst amacrine cell process contributes to direction selectivity in the retina was recently provided by a serial electron microscopic reconstruction of this circuit (Briggman et al, Nature, 2011). This reconstruction showed that individual starburst amacrine cell processes – rather than individual starburst cells – selectively wire to particular subtypes of DSGCs. In particular, the local orientation of the process dictates the size of the synapse – processes oriented parallel to the null direction of the

postsynaptic DSGC form a large (and therefore presumably strong) synapse, while processes oriented in other directions form smaller synapses or no synapses at all.

It is important to note that several other aspects of the retinal circuit contribute to the computation of direction selectivity (Borst & Euler, 2011; Wei & Feller, 2011). However, the aspect of asymmetric starburst amacrine cell wiring to DSGCs is the primary focus of the studies on the development of direction selectivity that are described below.

**Direction selectivity is present at eye-opening and forms independent of visual experience**

Several studies have concluded that direction selectivity is wired up at eye-opening and is independent of visual experience. Using large-scale multi-electrode array recordings (Elstrott et al., 2008) or single cell-attached recordings (Chan & Chiao, 2008; Chen, Weng, Deng, Xu, & He, 2009; Masland, 1977), researchers have detected robust On-Off directional responses before or at eye opening in mice and rabbits. This also holds true for mice that are dark-reared prior to eye-opening (Chan & Chiao, 2008; Elstrott et al., 2008). Similar results have been found for On-DSGCs (K. Yonehara et al., 2009). At this young age, both the excitatory inputs (Tian & Copenhagen, 2001) and the intrinsic excitability of retinal ganglion cells (Chen et al., 2008; Qu and Myhr, 2008; Sun et al., 2008) lack maturity, so the firing rate in the preferred direction is lower than that in adult animals. However, the firing rate in the null direction is as low as the rate in adult, indicating that the circuits mediating null-side inhibition are established early in development.

Support for this early establishment of direction selectivity was provided by a recent study in which direction selective responses were detected in the visual cortex of mice at eye-opening (Rochefort et al., 2011). In stark contrast, ferrets exhibit a direction selectivity in the cortex that occurs after eye-opening and does require visual experience (Li, Fitzpatrick, & White, 2006; Li, Van Hooser, Mazurek, White, & Fitzpatrick, 2008). Interestingly, in mouse visual cortex, the distribution of directional preference is not uniform at eye-opening, with a larger percentage of cells preferring anterior and dorsal motion direction over the opposite directions (Rochefort et al., 2011). This anisotropy mimics the distribution that has been reported in retinas where a larger percentage of cells prefer motion toward either the temporal or the ventral part of the retina (Elstrott et al., 2008). In adult rabbits, the ultimate distribution of DSGC preferred directions is unchanged even if the rabbits are raised in a visual environment consisting entirely of vertical stripes rotating in one direction (Daw & Wyatt, 1974). Together, these results show that the initial establishment of retinal direction selectivity in mice and rabbits occurs independent of visual experience.

**Transgenic mouse lines are used to study direction selectivity prior to maturation of the light response**.

Addressing the developmental events in the establishment of direction selectivity has been significantly hindered in the past because there was no reliable way to identify a DSGC without first measuring a light response. Since the synaptic connections fundamental to the

response become established before eye-opening and the emergence of visual function, identification of nascent DSGCs needs to be based on something other than the tuning curve.

The field was recently transformed by two technological breakthroughs. First, genetically altered mouse lines have been identified that express GFP selectively in certain DSGC subtypes, specifically On-DSGCs (K. Yonehara et al., 2009; Keisuke Yonehara et al., 2008), On-Off DSGCs (Huberman et al., 2009; Kay et al., 2011; Rivlin-Etzion et al., 2011; Trenholm, Johnson, Li, Smith, & Awatramani, 2011), and Off-DSGCs (Kay et al., 2011; I. Kim, Zhang, Yamagata, Meister, & Sanes, 2008; I.-J. Kim, Zhang, Meister, & Sanes, 2010). These mice have allowed the morphological characterization and identification of projection patterns from identified DSGCs (see Sanes 201 . Second, the technique of two-photon targeted recording has been applied to the retina. Typically, recording light responses from GFP-expressing retinal neurons requires illuminating the retina with light at a wavelength that is appropriate to excite GFP. However, this light also stimulates the photopigment, so it leads to rapid and irreversible bleaching of the light response. To avoid this, two-photon excitation based on infrared light has been used to visualize the neurons, since infrared light spares the photopigment and therefore the light response (Euler et al., 2009; Wei, Elstrott, & Feller, 2010). Using two-photon targeted recording on these lines of transgenic mice has enabled clear characterization of the light responses of identified subtypes of DSGCs.

One intriguing outcome of the above approaches is that some markers label specific subsets of DSGC subtypes. For example, SPIG1-GFP is expressed solely in On-DSGCs that prefer motion in the upward direction. Similarly, the BAC-transgenic mouse, where GFP is expressed under the type 4 dopamine receptor, expresses GFP in a subset of On-Off DSGCs that prefer motion in the posterior direction. These lines enable us to address two important questions: how do DSGCs divide into their respective subtypes during development, and is this process partially or fully under the control of genetic specification? By isolating GFP (+) populations of neurons by fluorescence-activated cell sorting (FACS), researchers can perform a molecular characterization of individual DSGC subtypes. Indeed, this method has identified several cell-surface markers that uniquely mark subtypes of On-Off DSGCs (Kay et al., 2011). Since these distinguishing markers are found prior to eye-opening, the different subtypes of On-Off DSGCs are thought to exist independent of visual experience (Kay et al., 2011). Studies such as these have just begun, but similar methods are likely to lead to insights on how individual subtypes are specified.


**Specific inhibitory circuits are established prior to eye-opening**

A fundamental component of the direction selective circuit is the asymmetric wiring of starburst amacrine cells to DSGCs. In the adult retina, this asymmetry has been determined by paired recordings between starburst amacrine cells and DSGCs – if a starburst amacrine cell is located on the null-side then there is stronger overall synaptic input than if the starburst amacrine cell is located on the preferred side. Recordings from DSGCs at eye-opening indicate that the null-side inhibition is in place at this early stage of development. The questions then arise – when and how does this asymmetry evolve during development? There are two options. On one

hand, the asymmetry could reflect a very specific synaptic connection between the null-side starburst amacrine cells and DSGCs at the point of synaptogenesis. On the other hand, the starburst amacrine cells could initially make GABAergic contacts with both preferred- and null-side DSGCs and through the course of development could either keep or strengthen only the null-side synapses.

This issue has been addressed using two methods. First, targeted paired recordings have been performed on transgenic mice in which both posterior-preferring DSGCs and starburst amacrine cells express GFP (Wei, Hamby, Zhou, & Feller, 2011). These mice are double transgenics that are a cross between the DRD4-GFP line and mGluRII-GFP line (which labels starburst amacrine cells). Though both starburst amacrine cells and DSGCs express GFP, they can be distinguished by their morphologies and their intracellular patterns of GFP expression. The recordings show that, as early as P4, inhibitory synapses between starburst amacrine cells and DSGCs are detected, and, until P7, DSGCs receive symmetric GABAergic input from starburst amacrine cells on both the preferred and null sides. However, by P14, the strength of the GABAergic conductance between DSGCs and null-side starburst amacrine cells increases several fold, while that between DSGCs and preferred-side starburst amacrine cells remains weak. Hence, the asymmetry of connectivity is thought to arise between P7 and P14.

The second method used to address the question of asymmetry development is that of using optogenetics to characterize the pattern of inhibitory synapses during development (Keisuke Yonehara et al., 2011). In these studies, channelrhodopsin (ChR) is expressed in a large percentage of the starburst amacrine cells in mice where ON-DSGCs express GFP. In adult, inhibitory currents in ON-DSGCs that are evoked by photostimulating the null side are larger than those evoked by photostimulating the preferred side. This ChR-evoked response in the ON DSGC is symmetric at P6 and sharply transitions to an asymmetric pattern at P8, indicating that this synaptic strengthening occurs over only a two-day period.

Neither of these methods was able to determine whether the developmental change in overall synaptic strength is due to changes in the number of synapses or to changes in the strength of individual synapses. However, they do both indicate that a subset of GABAergic synapses made between the two cell types are destined to be formed or strengthened during a relatively short time in development. The cellular mechanisms that underlie this synapse-specific formation and/or strengthening remain to be determined.

**Molecular specificity and dendritic arborization**

One likely set of mechanisms that underlies the specificity of direction selective circuit architecture involves the interplay of signaling molecules that dictate the connections between specific cell types. In this scenario, each subtype of DSGC expresses a particular molecule on its dendrites, and this molecule interacts with a cognate molecular partner expressed selectively on starburst amacrine cell processes that are oriented in the null direction of the partnering DSGC. Such hypotheses have been offered to explain how a circuit comprised of cells with symmetric morphology can wire in an asymmetric way. While the hunt for molecular players that might mediate the specific wiring of direction selective circuits is underway, the key molecular players

have not yet been identified. However, recent advances have hinted that the retina uses both cell-adhesion molecules and transmembrane guidance cues to establish these circuits.

The evidence that several cell adhesion molecules are involved in the development of retinal circuits is reviewed in (Fuerst & Burgess, 2009). One particular family of cell-adhesion molecules, the DSCAMs (Down Syndrome Cell Adhesion Molecule), has been shown to play a role in the laminar stratification (Yamagata & Sanes, 2008) of the retina, as well as in its mosaic spacing (Fuerst et al., 2009; Keeley et al., 2011). DSCAMs are members of the immunoglobulin superfamily and mediate both attractive and repulsive intercellular events, depending on the setting and species. In drosophila, DSCAMs are known to undergo extensive alternative splicing, giving rise to up to ~38,000 isoforms, and to control mosaic spacing, axonal tiling and branching, and synaptic specificity. The vertebrate homologs are far less diverse, consisting of only a handful of genes that do not undergo alternative splicing. Nevertheless, in chicken – a species that is not known to have DSGCs - deletion or mis-expression of DSCAMs and the closely related DSCAM-like and Sidekick molecules reveals that they collectively specify stratification and synaptic partner choice in the inner-plexiform layer (Yamagata & Sanes, 2008; Yamagata, Weiner, & Sanes, 2002). This contrasts with the case in mouse. There, deletion of DSCAMs or DSCAM-L does not alter lamination but these molecules do act as repulsive cues that prevent the adhesion of neurons of the same type, essentially acting to enforce proper mosaic spacing (Fuerst et al., 2009). Thus, in DSCAM KO mice, many neurons form aggregated clumps where previously they were evenly spaced. However, their dendrites still seek out and terminate in the proper sublaminae and associate with their normal synaptic partners. These findings indicate that lamination and mosaic spacing in mice are likely mediated by different factors. While this study did not specifically investigate the direction selective circuit, the preservation of dendritic targeting despite the gross disorganization of neuronal somas implies that DSCAMs do not help organize mammalian retinal circuits at the level of synapse specificity and therefore they are likely not responsible for wiring up specific direction selective connections.

Repulsive transmembrane guidance cues have also been implicated in playing a role in retinal lamination by a few very recent studies (Matsuoka, Chivatakarn et al., 2011; Matsuoka, Nguyen-Ba-Charvet et al., 2011). In these works, transmembrane semaphorins signal through the Plexin receptors and direct the processes of select subtypes of retinal neurons to specific sublaminae within the IPL via a process of repulsion. In particular, a subset of semaphorins (Sema5A and Sema5b) signals through its receptors (PlexinA1 and PlexinA3) and prevents dendrites from residing in the Off sublamina. Though knockouts of these signaling molecules impair Off visual responses, direction selectivity is not affected.

These recent studies implicate a variety of attractive and repulsive cues in establishing synaptic lamination patterns in the inner retina. At the time of these studies, markers for DSGCs were not easily available, having only been described in the last couple of years, so a phenotype for DSGCs has not yet been found. However, growing evidence indicates that individual direction selective subtypes do in fact express unique molecular profiles, including some transmembane adhesion molecules (Kay et al., 2011). Genetic profiling based on FACS sorted neurons has identified factors that are differentially expressed across various DSGCs neurons. Specifically, microarray analysis has obtained expression profiles for three of the four directional subtypes of On-Off DSGCs (nasal, ventral and dorsal), starburst amacrine cells and non-direction

selective RCGs. Some of these differentially expressed markers are molecules with an extracellular site of action and therefore may play a role in mediating intercellular interactions. These include collagen 25a1 (Col25a1), cadherin 6 (Cdh6) and matrix-metalloprotease 17 (Mmp17). Col25a1 and Cdh6 are expressed only in subtypes that prefer vertical motion (ventral and dorsal), while Mmp17 is expressed in subtypes that prefer nasal motion. Another transcript, CART (cocaine and amphetamine related transcript), is expressed by all DSGC subtypes, but not by any other retinal neurons. Of all the retinal neurons, only starburst amacrine cells express both Col25a1 and Cdh6, consistent with the idea that they mediate starburst amacrine cell-DSGC interactions. Subsequent studies will be required to test if these candidates play a role in the development of direction selective circuits, but these findings provide compelling evidence that genetic molecular factors likely play a large role in specifying certain elements of these circuits.

Insights into whether or not the circuits that meditate direction selectivity are established by molecular interactions can be found by examining the development of dendritic stratification and pruning. An accepted hypothesis is that if, during development, dendrites over-arborize and then prune, this process is probably influenced by neural activity; in contrast, if dendrites simply grow in well-defined strata, their lamination is probably determined primarily by molecular interactions. The overall size of dendrites is thought to be a consequence of activity and of molecular interactions among dendrites from the same cell type (for reviews, see Reese, Keeley, Lee, & Whitney, 2011; Tian, 2011). Kim et al. (I.-J. Kim et al., 2010) found that one subtype of DSGC, the Off-DSGC, over-arborizes within the IPL so that its dendrites enter and remain in the On-sublamina during the first postnatal week, but are absent at eye-opening. In contrast, dendrites of bistratified RGCs are narrow even at the earliest ages that they are observed (I.-J. Kim et al., 2010; Stacy & Wong, 2003). However, other non-direction selective subtypes show a far more dynamic process of innervation, with original overshooting or diffuse branching that is pruned or rearranged during the period between P5 and P13. Indeed, there appears to be no general rule for which subtypes undergo pruning and which do not (Tian, 2008, 2011), and future studies will be required to determine the role of molecular interactions in establishing directional circuits.

**A role for retinal waves in the establishment of direction selectivity?**

Does neural activity play a role in the development of direction selectivity? The presence, at eye-opening, of direction selective responses and asymmetric wiring of inhibitory synapses, even in dark-reared animals, indicates that sensory experience does not play a major role. However, prior to eye-opening, retinal waves provide a robust source of highly structured activity and could potentially serve as a 'proxy' for a moving stimulus in the pre-visual retina. These retinal waves are instructive for patterning the projections of retinal ganglion cells to their retinorecipient targets (Huberman, Feller, & Chapman, 2008; Xu et al., 2010). Thus, they are attractive candidates for investigation in direction selectivity for three key reasons: (1) waves are present during the maturation of synapses between many retinal cell types, including the period of null-side synapse strengthening described above; (2) waves correlate the depolarization of neighboring cell types in the inner retina, including starburst amacrine cells and DSGCs (Elstrott & Feller, 2010), and therefore could possibly drive activity-dependent synaptic strengthening or

synaptic refinement; (3) waves have been shown to have a directional bias (Elstrott & Feller, 2010; Stafford, Sher, Litke, & Feldheim, 2009).

To determine the role of retinal waves in establishing direction selectivity, investigators have employed a number of approaches. Intraocular injections of a voltage-gated sodium channel blocker (tetrodotoxin, TTX), a GABAA receptor agonist (muscimol), GABAA receptor antagonists (biccululline methiodide, SR95531/gabazine), or a cholinergic receptor agonist (epibatidine) (L. Sun, Han, & He, 2011; Wei et al., 2011) all fail to prevent the development of retinal direction selectivity. In addition, knockout mice that lack normal retinal waves during the first postnatal week maintain their direction selective responses. However, these are all negative results, meaning they show activity manipulations that do not alter the development of direction selectivity. Thus, future experiments based on targeted genetic manipulations will be needed to address more specific hypotheses on the role of neural activity in establishing various aspects of the circuit that mediates direction selectivity.

**Summary**:

The development of direction selectivity is a new and growing field with many unanswered questions. Although several studies indicate that direction selectivity is present at eye-opening, it is not yet known if this represents a mature state of the system. For example, the optokinetic reflex, a visually guided behavior mediated by On-direction selective cells (Yoshida et al., 2001), is not mature for two weeks after birth in rodents (Faulstich, Onori, & du Lac, 2004) and for several weeks in primates (Distler & Hoffmann, 2011). Whether this slow maturation reflects maturation within the retina or of circuits downstream is not yet known. Moreover, though some functional retinal mosaics are established at eye-opening (Anishchenko et al., 2010), whether or not this is the case for direction selective cells is also not known. Finally, the relative role of activity and molecular interactions in all of these maturational processes has yet to be established. With the advent of an ever-growing number of genetic and imaging tools, we anticipate that the years to come will reveal/herald tremendous progress in this field.

**References:**

Anishchenko, A., Greschner, M., Elstrott, J., Sher, A., Litke, A. M., Feller, M. B., et al. (2010). Receptive     field mosaics of retinal ganglion cells are established without visual experience. J Neurophysiol, 103(4),    1856-1864.

Berson, D. M. (2008). Retinal ganglion-cell types and their central projections. In R. H. Masland & T. D. Albright (Eds.), The Senses: A Comprehensive Reference (Vol. 1, pp. 491-520). San diego, CA: Academic press.

Borst, A., & Euler, T. (2011). Seeing things in motion: models, circuits, and mechanisms. Neuron, 71(6), 974-994.

Chan, Y.-C., & Chiao, C.-C. (2008). Effect of visual experience on the maturation of ON-OFF direction selective ganglion cells in the rabbit retina. Vision Res, 48(23-24), 2466-2475.

Chen, M., Weng, S., Deng, Q., Xu, Z., & He, S. (2009). Physiological properties of direction-selective ganglion cells in early postnatal and adult mouse retina. J Physiol, 587(Pt 4), 819-828.

Daw, N. W., & Wyatt, H. J. (1974). Raising rabbits in a moving visual environment: an attempt to modify directional sensitivity in the retina. J Physiol, 240(2), 309-330.

Demb, J. B. (2007). Cellular mechanisms for direction selectivity in the retina. Neuron, 55(2), 179-186.

Distler, C., & Hoffmann, K. P. (2011). Visual pathway for the optokinetic reflex in infant macaque monkeys. J Neurosci, 31(48), 17659-17668.

Elstrott, J., Anishchenko, A., Greschner, M., Sher, A., Litke, A. M., Chichilnisky, E. J., et al. (2008). Direction selectivity in the retina is established independent of visual experience and cholinergic retinal waves. Neuron, 58(4), 499-506.

Elstrott, J., & Feller, M. B. (2009). Vision and the establishment of direction-selectivity: a tale of two circuits. Curr Opin Neurobiol, 19(3), 293-297.

Elstrott, J., & Feller, M. B. (2010). Direction-selective ganglion cells show symmetric participation in retinal waves during development. J Neurosci, 30(33), 11197-11201.

Euler, T., Detwiler, P. B., & Denk, W. (2002). Directionally selective calcium signals in dendrites of starburst amacrine cells. Nature, 418(6900), 845-852.

Euler, T., Hausselt, S. E., Margolis, D. J., Breuninger, T., Castell, X., Detwiler, P. B., et al. (2009). Eyecup scope--optical recordings of light stimulus-evoked fluorescence signals in the retina. Pflugers Arch, 457(6), 1393-1414.

Faulstich, B. M., Onori, K. A., & du Lac, S. (2004). Comparison of plasticity and development of mouse optokinetic and vestibulo-ocular reflexes suggests differential gain control mechanisms. Vision Res, 44(28), 3419-3427.

Ford, K. J., Felix, A. L., & Feller, M. B. (2012). Cellular mechanisms underlying spatiotemporal features of cholinergic retinal waves. J Neurosci, 32(3), 850-863.

Fuerst, P. G., Bruce, F., Tian, M., Wei, W., Elstrott, J., Feller, M. B., et al. (2009). DSCAM and DSCAML1 function in self-avoidance in multiple cell types in the developing mouse retina. Neuron, 64(4), 484-497.

Fuerst, P. G., & Burgess, R. W. (2009). Adhesion molecules in establishing retinal circuitry. Curr Opin Neurobiol, 19(4), 389-394.

Huberman, A. D., Feller, M. B., & Chapman, B. (2008). Mechanisms underlying development of visual maps and receptive fields. Annu Rev Neurosci, 31, 479- 509.

Huberman, A. D., Wei, W., Elstrott, J., Stafford, B. K., Feller, M. B., & Barres, B. A. (2009). Genetic identification of an On-Off direction-selective retinal ganglion cell subtype reveals a layer-specific subcortical map of posterior motion. Neuron, 62(3), 327-334.

Kay, J. N., De la Huerta, I., Kim, I. J., Zhang, Y., Yamagata, M., Chu, M. W., et al. (2011). Retinal ganglion cells with distinct directional preferences differ in molecular identity, structure, and central projections. J Neurosci, 31(21), 7753- 7762.

Keeley, P. W., Sliff, B., Lee, S. C., Fuerst, P. G., Burgess, R. W., Eglen, S. J., et al. (2011). Neuronal clustering and fasciculation phenotype in dscam- and bax-deficient mouse retinas. J Comp Neurol.

Kim, I., Zhang, Y., Yamagata, M., Meister, M., & Sanes, J. (2008). Molecular identification of a retinal cell type that responds to upward motion. Nature, 452(7186), 478-482.

Kim, I.-J., Zhang, Y., Meister, M., & Sanes, J. R. (2010). Laminar Restriction of Retinal Ganglion Cell Dendrites and Axons: Subtype-Specific Developmental Patterns Revealed with Transgenic Markers. J. Neurosci., 30(4), 1452-1462.

Li, Y., Fitzpatrick, D., & White, L. E. (2006). The development of direction selectivity in ferret visual cortex requires early visual experience. Nat Neurosci, 9(5), 676-681.

Li, Y., Van Hooser, S., Mazurek, M., White, L. E., & Fitzpatrick, D. (2008). Experience with moving visual stimuli drives the early development of cortical direction selectivity. Nature, 456(7224), 952-956.

Masland, R. H. (1977). Maturation of function in the developing rabbit retina. J Comp Neurol, 175(3), 275-286.

Matsuoka, R. L., Chivatakarn, O., Badea, T. C., Samuels, I. S., Cahill, H., Katayama, K., et al. (2011). Class 5 transmembrane semaphorins control selective Mammalian retinal lamination and function. Neuron, 71(3), 460-473.

Matsuoka, R. L., Nguyen-Ba-Charvet, K. T., Parray, A., Badea, T. C., Chedotal, A., & Kolodkin, A. L. (2011). Transmembrane semaphorin signalling controls laminar stratification in the mammalian retina. Nature, 470(7333), 259-263.

Reese, B. E., Keeley, P. W., Lee, S. C., & Whitney, I. E. (2011). Developmental plasticity of dendritic morphology and the establishment of coverage and connectivity in the outer retina. Dev Neurobiol.

Rivlin-Etzion, M., Zhou, K., Wei, W., Elstrott, J., Nguyen, P. L., Barres, B. A., et al. (2011). Transgenic mice reveal unexpected diversity of on-off direction-selective retinal ganglion cell subtypes and brain structures involved in motion processing. J Neurosci, 31(24), 8760-8769.

Rochefort, N. L., Narushima, M., Grienberger, C., Marandi, N., Hill, D. N., & Konnerth, A. (2011). Development of direction selectivity in mouse cortical neurons. Neuron, 71(3), 425-432.

Rockhill, R. L., Daly, F. J., MacNeil, M. A., Brown, S. P., & Masland, R. H. (2002). The diversity of ganglion cells in a mammalian retina. J Neurosci, 22(9), 3831-3843.

Stacy, R. C., & Wong, R. O. L. (2003). Developmental relationship between cholinergic amacrine cell processes and ganglion cell dendrites of the mouse retina. J Comp Neurol, 456(2), 154-166.

Stafford, B. K., Sher, A., Litke, A. M., & Feldheim, D. A. (2009). Spatial-temporal patterns of retinal waves underlying activity-dependent refinement of retinofugal projections. Neuron, 64(2), 200-212.

Sun, L., Han, X., & He, S. (2011). Direction-selective circuitry in rat retina develops independently of GABAergic, cholinergic and action potential activity. PLoS One, 6(5), e19477.

Sun, W., Deng, Q., Levick, W. R., & He, S. (2006). ON direction-selective ganglion cells in the mouse retina. J Physiol, 576(Pt 1), 197-202.

Sun, W., Li, N., & He, S. (2002). Large-scale morphological survey of mouse retinal ganglion cells. The Journal of Comparative Neurology, 451(2), 115.

Tian, N. (2008). Synaptic activity, visual experience and the maturation of retinal synaptic circuitry. J Physiol, 586(Pt 18), 4347-4355.

Tian, N. (2011). Developmental mechanisms that regulate retinal ganglion cell dendritic morphology. Dev Neurobiol, 71(12), 1297-1309.

Tian, N., & Copenhagen, D. R. (2001). Visual deprivation alters development of synaptic function in inner retina after eye opening. Neuron, 32(3), 439-449.

Trenholm, S., Johnson, K., Li, X., Smith, R. G., & Awatramani, G. B. (2011). Parallel mechanisms encode direction in the retina. Neuron, 71(4), 683-694.

Vaney, D. I., & Taylor, W. R. (2002). Direction selectivity in the retina. Curr Opin Neurobiol, 12(4), 405-410.

Wei, W., Elstrott, J., & Feller, M. B. (2010). Two-photon targeted recording of GFP-expressing neurons for light responses and live-cell imaging in the mouse retina. Nat Protoc., 5(7), 1347-1352.

Wei, W., & Feller, M. B. (2011). Organization and development of direction-selective circuits in the retina. Trends Neurosci, 34(12), 638-645.

Wei, W., Hamby, A. M., Zhou, K., & Feller, M. B. (2011). Development of asymmetric inhibition underlying direction selectivity in the retina. Nature, 469(7330), 402-406.

Xu, H. P., Furman, M., Mineur, Y. S., Chen, H., King, S. L., Zenisek, D., et al. (2010). An instructive role for patterned spontaneous retinal activity in mouse visual map development. Neuron, 70(6), 1115-1127.

Yamagata, M., & Sanes, J. R. (2008). Dscam and Sidekick proteins direct lamina- specific connections in vertebrate retina. Nature, 451, 465.

Yamagata, M., Weiner, J. A., & Sanes, J. R. (2002). Sidekicks: synaptic adhesion molecules that promote lamina-specific connectivity in the retina. Cell, 110, 649.

Yonehara, K., Balint, K., Noda, M., Nagel, G., Bamberg, E., & Roska, B. (2011). Spatially asymmetric reorganization of inhibition establishes a motion-sensitive circuit. Nature, advance online publication.

Yonehara, K., Ishikane, H., Sakuta, H., Shintani, T., Nakamura-Yonehara, K., Kamiji, N., et al. (2009). Identification of Retinal Ganglion Cells and Their Projections Involved in Central Transmission of Information about Upward and Downward Image Motion. PLoS ONE, 4(1), e4320.

Yonehara, K., Shintani, T., Suzuki, R., Sakuta, H., Takeuchi, Y., Nakamura-Yonehara, K., et al. (2008). Expression of SPIG1 Reveals Development of a Retinal Ganglion Cell Subtype Projecting to the Medial Terminal Nucleus in the Mouse. PLoS ONE, 3(2), e1533.

Yoshida, K., Watanabe, D., Ishikane, H., Tachibana, M., Pastan, I., & Nakanishi, S. (2001). A key role of starburst amacrine cells in originating retinal directional selectivity and optokinetic eye movement. Neuron, 30(3), 771-780.

**Figure I-1: Direction selective retinal circuit and ganglion cell types.**

A. Schematic of the retinal circuit that mediates direction selectivity. The direction selective ganglion cell (g) projects dendrites into the ON and OFF halves (or sublaminae) of the retina's inner synaptic layer. The dendrites in each sublamina receive synapses from the corresponding type of bipolar cell (b) that is relaying signals from cone photoreceptors (c), and starburst amacrine cells (s). (from Demb, 2007)

B. Live two-photon images of a P10 On-Off-DSGC (left), a P9 On-DSGC (middle), and a P11 Off-DSGC (right), all before eye opening. The On-Off- and On-DSGCs were filled with Alexa 594 before imaging. (from Elstrott & Feller, 2010)
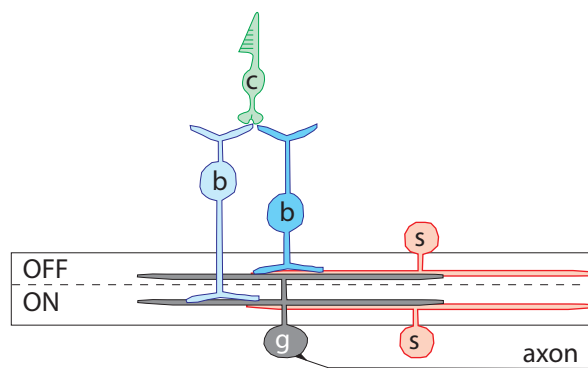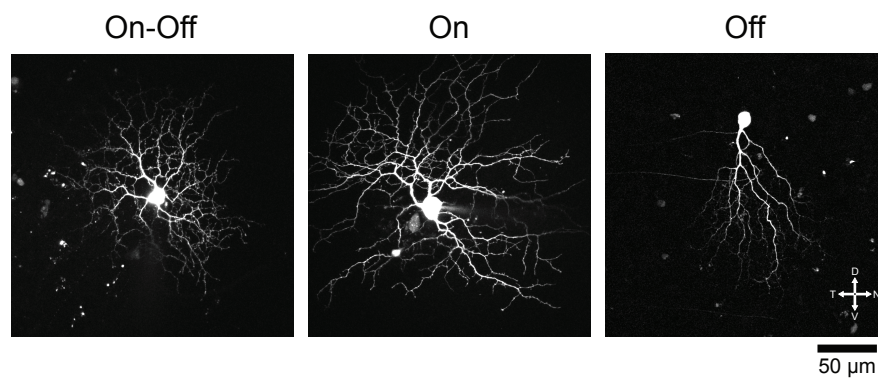
**A**



**B**

| On-Off | On | Off |



50 µm

**Figure I-2: Responses of On-Off DSGCs to moving gratings reveal strong direction selectivity in the adult and P14 dark reared mouse.**

A&C. Polar-plot of the mean spike rate across five repetitions in response to motion in 16 directions. Spike traces for all directions are shown for one period of the moving grating. The arrow indicates the mean preferred direction of the cell. Firing rate is calculated as the total number of spikes divided by the stimulus duration (10 sec). Adult: n = 31 cells; P14 dark reared: n = 15 cells.

B & D. The preferred directions of all On-Off DSGCs within one animal preparation. These directions fall clearly into four groups along the cardinal directions for the adult (B), but are more variable at P14 (D). The preferred direction for each cell is shown as the vector sum of the response, so the length of each line indicates the normalized response magnitude.

E. The symmetry of preferred directions along a given axis (temporal-nasal or ventral-dorsal) is determined by calculating the fraction of cells that fall in one quadrant along the axis (e.g., temporal) versus the fraction of cells that fall in the opposite quadrant (e.g., nasal). A perfectly symmetric axis would show 50% of the cells in opposite quadrants. The thick black bars show the actual distribution of cells along the axes for adult and P14. The shaded gray regions show the 95% confidence interval around each value based on resampling of the adult and P14 distributions. These data indicate that there is a nonuniform distribution of cells among the four cardinal directions. In addition, the representation of opposite directions along the same axis was strongly biased, with nasal and dorsal quadrants significantly underrepresented compared to their opposites.

F. A comparison of adult and P14 distributions of preferred directions on a quadrant-by-quadrant basis. These data indicate that the relative representation of the nasal and ventral directions was significantly changed between P14 and adult. With a uniform distribution, each quadrant would encompass 25% of the cells. (From Elstrott et al, 2008).

**A  Adult - light reared**

Dorsal
25 Hz
Temporal
Nasal
Ventral

**B**

Dorsal
0.5
Temporal
Nasal
Ventral

**C  P14 - dark reared**

Dorsal
7.5 Hz
Temporal
Nasal
Ventral

1 s

**D**

Dorsal
0.5
Temporal
Nasal
Ventral

**E**

Adult    P14

fraction of cells

T | V    T | V
N | D    N | D

**F**

adult fraction of cells

nasal *
dorsal
temporal
ventral *

P14 fraction of cells
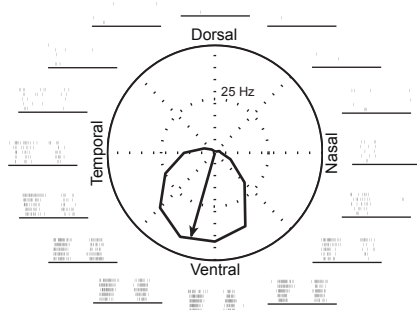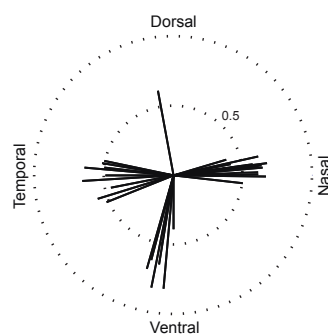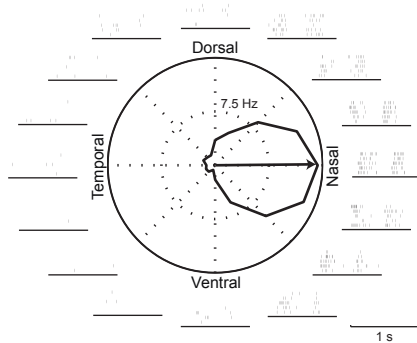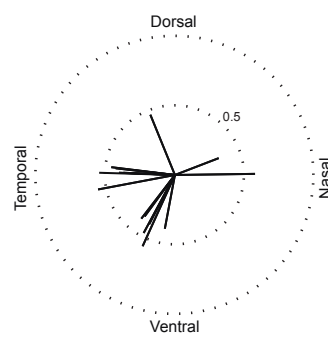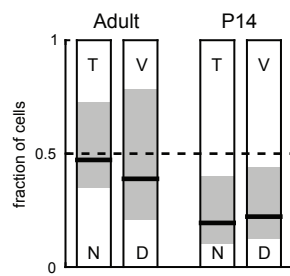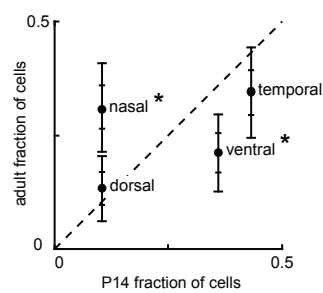
**Figure I-3: Synaptically connected, dye-filled starburst amacrine cell–DSGC pairs at P4, P7 and P30.**

On the left are null-side pairs where the starburst amacrine cells (filled with green fluorescent dye) are located on the null side of the DSGCs (filled with red fluorescent dye). On the right are preferred-side pairs. Scale bar: 50 μm.

(From (Wei et al., 2011)

Null side ←——————— Preferred side
Preferred direction



P4

P7

P30
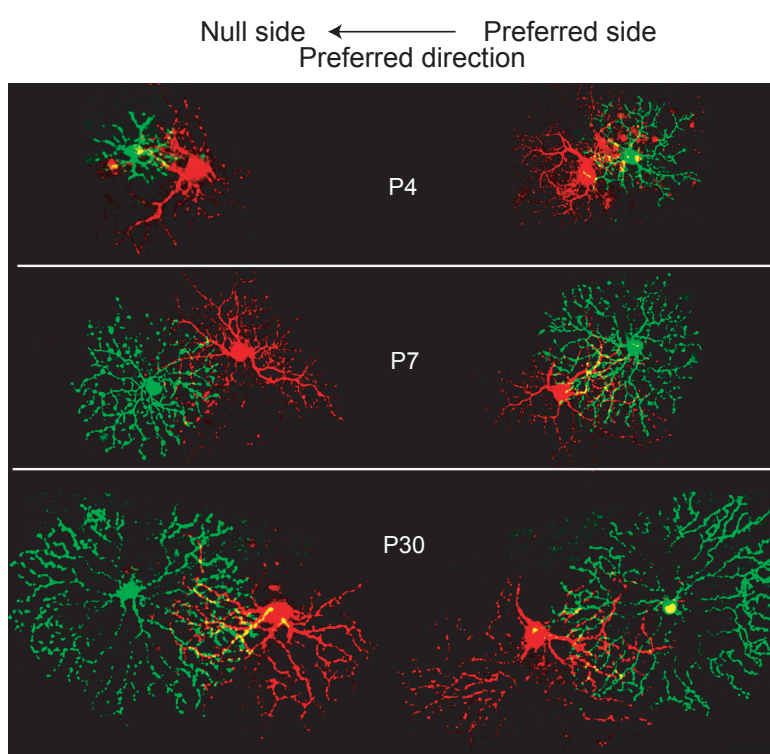
**Figure I-4: DSGCs and starburst amacrine cells are depolarized by retinal waves**

A. Left:  Live fluorescence imaging (top) of P5 Spig1 retina (where GFP is expressed in On-DSGCs) bolus loaded with the calcium indicator OGB-1 AM and the same retina with the On-DSGC targeted for cell-attached recording configuration (bottom).

Right: ΔF/F trace reveals periodic retinal waves that pass over a 200 x200 μm region centered on the On-DSGC cell, and the spike bursts below are elicited from the cell during these waves. Inset shows a magnified view of the spikes evoked by a single wave.  (From (Elstrott & Feller, 2010))

B. Left: Live fluorescence image of a mGluR2-GFP retina (top) and the same retina with the starburst amacrine cell targeted for whole-cell recording and filled with Alexa 568 (bottom). Scale bar: 10 μm.

Right: Current-clamp perforated-patch recording from the starburst amacrine cell shows wave-induced depolarizations followed by sAHPs. Inset shows a magnified view of the calcium spikes during a wave-induced depolarization.  (from Ford, Felix, & Feller, 2012)

## A  Direction selective ganglion cells



ΔF/F

5%

100 s

500 ms

20 μm
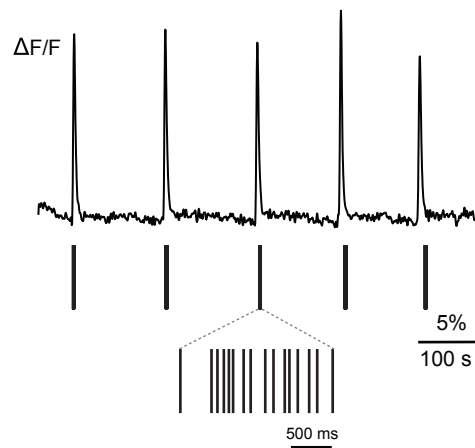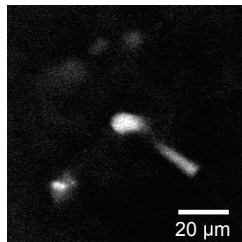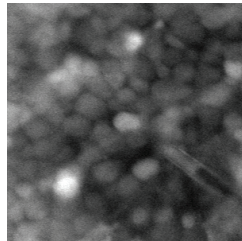
## B Starburst amacrine cells



-50mV

10mV

30s

1s
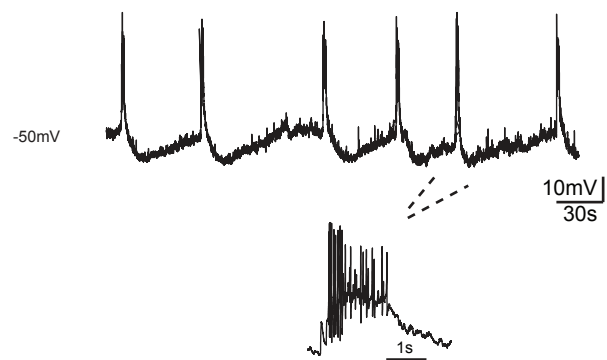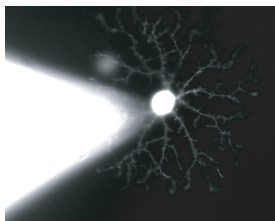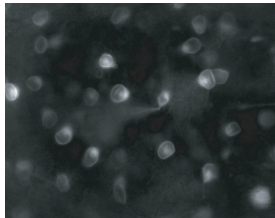
**Figure I-5: Retinas that receive daily intraocular injections of GABA-A receptor antagonists display normal DSGCs.**

A. DSGC response to the onset and termination of a stationary flashing spot. B. Directional responses of this same DSGC to a rectangle moving in 12 directions. The preferred direction is represented by the arrow in the middle of the polar plot. The traces of action potentials that surround this plot are the responses evoked by motion in each direction. C. Asymmetric synaptic inputs are recorded when the membrane potential is held at −65 mV and 0 mV. Much larger inhibitory inputs are observed when the visual stimulus moves in the null direction (left) as opposed to preferred direction (right). D. Dendritic morphology of the recorded cell. A section of the dendritic field is enlarged to show the clear segregation between ON (E) and OFF (F) layers. G. These dendrites tightly co-stratify with the cholinergic processes of starburst amacrine cells (red). Scale bar: 30 µm. (From (L. Sun et al., 2011).
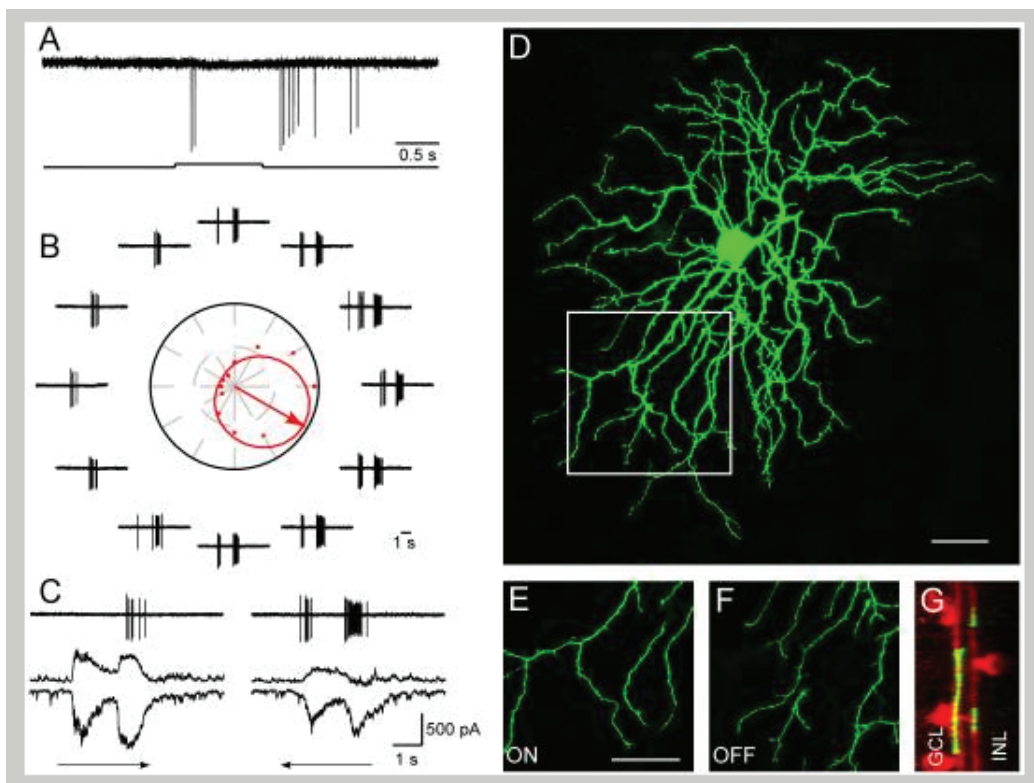
## II. Development of asymmetric inhibition underlying direction selectivity in the retina

## Abstract

Establishing precise synaptic connections is crucial to the development of functional neural circuits. The direction selective circuit in the retina relies upon highly selective wiring of inhibitory inputs from starburst amacrine cells (SACs)[1] onto four subtypes of On-Off direction selective ganglion cells (DSGCs), each preferring motion in one of four cardinal directions[2]. It has been reported in rabbit that the SACs on the null side of DSGCs form functional GABAergic synapses, whereas those on the preferred side do not3. However, it is not known how the asymmetric wiring between SACs and DSGCs is established during development. Using transgenic mice with cell type-specific labeling, we found that during the first postnatal week the synaptic connections from SACs to DSGCs were of equal strength, regardless of whether the SAC was located on the DSGC's preferred or null side. However, by the end of the second postnatal week the strength of the synapses made from SACs on the null side of a DSGC significantly increased while those made from SACs located on the preferred side remained constant. Blocking retinal activity by intraocular injections of muscimol during this period did not alter the development of direction selectivity. Hence, the asymmetric inhibition between the SACs and DSGCs is achieved by a developmental program that specifically strengthens the GABAergic inputs from SACs located on the null side, in a manner not dependent on neural activity.

## Introduction

The ability to detect motion in the visual scene is a fundamental computation in the visual system that is first performed in the retina. Motion direction is encoded by DSGCs, which fire a maximum number of action potentials during movement in their preferred direction, but fire minimally for movement in the opposite, or "null",
direction[4, 5]. In the mammalian retina, the directional preference of an On-Off DSGC is caused by asymmetric inhibitory inputs: movement in the null direction causes strong inhibition that effectively shunts light-evoked excitatory inputs. Indeed, blocking GABA-A receptors abolishes the directionality of DSGCs by increasing spiking in response to null-direction motion[6-8]. Null-side inhibition is thought to arise from SACs, because 1) their processes cofasciculate with DSGC dendrites[9-11], where they form direct GABAergic synapses[3] and 2) ablation of SACs eliminates the directional preference of DSGCs[12, 13].

How SAC-DSGC synapses are organized to provide asymmetric inhibition has been an intriguing but elusive question since no apparent asymmetry is detected in the morphology or the distribution of synaptic markers in DSGCs and SACs[14-17]. The first and only piece of evidence for the synaptic basis of asymmetric inhibition came from a functional study between SAC and DSGC pairs in the rabbit retina[3], which suggested that SACs on the null side provide inhibitory inputs to the DSGCs, but those on the preferred side do not. Whether this asymmetric inhibition

exists in the mouse is not known.  In addition, since the directional preference of an On-Off DSGC is present by eye-opening[18-20] little is known about the developmental program that shapes the SAC-DSGC synapses because the identification of DSGCs and their preferred directions is almost impossible before the onset of the light response.

## Results and Discussion

Here we use paired recordings and morphological reconstructions from a double transgenic mouse line that selectively expresses two variants of GFP in SACs and nasal-preferring On-Off DSGCs (nDSGCs) to characterize the organization and the development of the precise wiring between SACs and DSGCs. These mice were generated by crossing two existing lines; 1) Drd4-GFP mice, where Drd4 promoter-driven GFP expression is restricted to nDSGCs[21]; and 2) mGluR2-GFP mice, where a membrane-tethered human interleukin 2-GFP fusion protein is expressed specifically in SACs in the retina (Fig. 1a)[22].

To detect functional GABAergic synapses between SACs and DSGCs, we performed targeted whole-cell voltage-clamp recordings from SAC-DSGC pairs in whole-mount retinas. To isolate GABAergic synapses, paired recordings were carried out in the presence of drugs that block excitatory synaptic transmission (Fig. 1b). Alexa dyes were included in the recording pipettes for visualizing the dendritic morphology of the recorded pairs (Fig. 1c). Only pairs with overlapping dendritic fields were used for analysis.

Paired recordings were carried out in P4, P7, P14 and adult mice. At P4, GABAergic currents elicited by SAC depolarization were detected in nDSGCs in 64% of pairs (16 out of 25 pairs, Fig. 1b,d), indicating that synapse formation between SACs and nDSGCs occurred prior to and during the first postnatal week, confirming previous findings11. By P7, nearly all pairs showed unitary GABAergic connections (P7: 85%, 29 out of 34 pairs) and this high level of connectivity persisted into adulthood (P14-48: 91%, 41 out of 45 pairs; Fig. 1d).  The evoked response was completely blocked by the GABA-A antagonist gabazine (5 μM, n= 4, data not shown), indicating that the GABAergic transmission between SACs and nDSGCs is mediated by GABA-A receptors. Note, the finding that connections were readily detected between SACs located on the preferred side of DSGCs in the adult is in contrast to previous findings in the rabbit.[3]

Though SACs located on both the preferred and null side formed GABAergic synapses with DSGCs, a significant asymmetry in the unitary synaptic strength emerged along the null-preferred axis during the second postnatal week.  Synaptic strength was quantified as the GABA-A receptor-mediated whole cell conductance. These measurements were conducted from the null and the preferred side pairs that had a similar amount of overlap between SAC processes and DSGC dendrites. Surprisingly, at P4 and P7, the GABA-mediated conductance from both groups was similar (Fig. 2). However, a significant increase in unitary conductance was detected in the null side pairs, but not in the preferred side pairs in retinas P14 and older (Fig. 2).   Hence the establishment of the direction selective circuits is mediated by an asymmetric increase in the strength of the unitary conductance between starburst amacrine cells and DSGCs in the week prior to eye-opening.

The difference in GABAergic conductance from the null and preferred side SACs prompted us to examine two hypotheses regarding the mechanisms underlying this strengthening. First we tested whether this functional asymmetry was correlated with the number or quality of contacts between SACs and nDSGCs, indicating a preferential adhesion between SACs located on the nullside and DSGCs3. After electrophysiological recording, the dendritic arbors of the synaptically connected, Alexa dye-filled SAC-nDSGC pairs from P14-48 were imaged live with a two-photon microscope and reconstructed with Neurolucida (Fig. 3a). We examined the overlapping region between the nDSGC dendrites and the distal portion (roughly outer third) of the SAC processes enriched in varicosities, which are the sites of neurotransmitter release[10]. Crossing points between distal SAC processes and nDSGC dendrites were defined as "contacts" (Fig. 3a, inset). A subset of contacts exhibited cofasciculation, which were defined as 2 μm segments along which the processes from the two cells remained in contact (Fig. 3a, inset). The null side and the preferred side SAC-nDSGC pairs showed a similar density of contacts (Fig. 3b) and cofasciculations (Fig. 3c). No asymmetry was found when the entire SAC processes were included for the above analysis (Fig. 5). Therefore, the functional asymmetry in GABAergic synapses does not involve selective membrane adhesion between nullside SAC processes and DSGC dendrites.

Second, we tested whether spontaneous retinal activity during the second postnatal week played a role in the establishment of direction selectivity. DSGCs are depolarized by retinal waves and therefore activity could potentially influence the synapse strengthening[23]. To this end, we first confirmed that the GFP-labeled nDSGCs in the Drd4-GFP mice exhibited a clear preference for nasal motion at eye opening (Fig. 4a) that was sensitive to the GABA-A receptor antagonist gabazine (Fig. 6), with a direction selective index (DSI) similar to those recorded in the adult (Fig. 4b). We then injected muscimol, a GABA-A receptor agonist, intravitreally into Drd4-GFP mice to block all spontaneous and evoked neural activity in the retina[24]. In the presence of muscimol, evoked synaptic transmission from SACs to nDSGCs and spontaneous activity in both cell types were completely suppressed (Fig. 4c and Fig. 7a and b). The effectiveness of muscimol injection at blocking activity in vivo was confirmed by examining eye-specific segregation of retinogeniculate projections, which is an independent measure of retinal activity (Fig. 8c and d), as well as the persistence of fluorescently labeled muscimol in the retina at 48 hours post injection (Fig. 7e).

We assessed the responses of nDSGCs to stationary flashes and drifting gratings in P14-15 mice that had received repeated muscimol injections in the second postnatal week. Muscimol treatment did not prevent the development of direction-selective responses or significantly reduce directional tuning of nDSGCs (Fig. 4a and b). Normal On and Off light responses were also present in the muscimol-treated group, although there was an increase in the number of cells that did not respond to gratings in the muscimol-treated group (Fig. 8).

While muscimol suppresses all neural activity in the retina, it also tonically activates GABA-A receptors. To test the hypothesis that GABA-A receptor activation is required for the development of direction selectivity, we performed intravitreal injections of the GABA-A receptor antagonist gabazine in Drd4-GFP mice during the second postnatal week. Gabazine treatment did not prevent the development of direction-selective responses of GFP+ cells to

drifting gratings (Fig. 4 a and b). Therefore, the development of direction selectivity arises independent of spontaneous retinal activity.

To begin to explore the synaptic basis of this increase in conductance between nullside SACs and DSGCs, we recorded the spontaneous IPSCs from nDSGCs at P7 and P14. We found a significant increase in the frequency and no significant change in the amplitude of the GABAergic IPSCs, though there was a trend toward larger IPSC amplitudes at P14 (Fig. 8). This result is consistent with the hypothesis that the stronger GABAergic unitary conductance for the null-side pairs is primarily due to increased number of functional GABAergic synapses. However, we cannot distinguish whether the spontaneous IPSCs originate from the null or preferred side SACs. Further studies are required to determine the relative role of increases in synapse number versus synapse strength in the increase in the unitary conductance between nullside SAC and DSGCs.

Our study demonstrates that asymmetric inhibition arises during the second postnatal week through selective strengthening of the GABAergic conductance from SACs on the null side of DSGCs. Morphological analysis revealed a similar degree of dendritic contact and cofasciculation between SAC on the null or preferred side, indicating that the synapse development is dissociated from physical encounters between SAC processes and DSGC dendrites, as was recently found in barrel cortex[25].

In addition, we found that blocking depolarization-induced activity or GABA-A receptor activation did not affect the establishment of direction selectivity in the retina, in sharp contrast to direction-selective cells in the visual cortex[26]. This finding lends support to previous studies showing that early visual experience[18-20] or cholinergic retinal waves[20] are not involved in establishing retinal direction selectivity. Therefore, the mechanism underlying the development of retinal direction selectivity is an asymmetric increase in the strength of the inhibitory unitary conductance between SACs and DSGCs in the week prior to eye-opening, without the establishment of asymmetrical dendritic contacts and independent of spontaneous neural activity.

## Experimental Procedures:

### Mice

DRD4-GFP mice in the Swiss Webster background were obtained from MMRRC (http://www.mmrrc.org/strains/231/0231.html)21, and mGluR2-GFP mice were a gift from Shigatada Nakanishi, Osaka. Both strains were backcrossed to the C57/Bl6 background in our laboratory. The DRD4-GFP/mGluR2-GFP double transgenic mice were obtained by crossing the two single transgenic lines.

### Whole-cell patch clamp recording

Single or dual whole-cell voltage-clamp recordings from SACs and nDSGCs were performed in oxygenated ACSF at 32–34°C containing (in mM): 119.0 NaCl, 26.2 NaHCO3, 11 glucose, 2.5 KCl, 1.0 K2HPO4, 2.5 CaCl2, 1.3 MgCl2, 0.05 APV, 0.02 DNQX and 0.008 D. Recording

electrodes of 3-5 M were filled with an internal solution containing (in mM): 110 CsMeSO4, 2.8 NaCl, 4 EGTA, 5 TEA-Cl, 4 adenosine 5′-triphosphate (magnesium salt), 0.3 guanosine 5′-triphosphate (trisodium salt), 20 HEPES and 10 phosphocreatine (disodium salt), 0.025 Alexa 488 (for SACs), 0.025 Alexa 594 (for nDSGCs), pH 7.25. Data were acquired using pCLAMP 10 recording software and a Multiclamp 700A amplifier (Molecular Devices), filtered at 4 kHz, and digitized at a sampling rate of 10 kHz. GABAergic whole-cell conductance was calculated from the linear portion of the current-voltage (I-V) curve for the SAC-evoked currents in nDSGCs and analyzed using Matlab software.

### *Two-photon targeted loose-patch recording of GFP+ neurons for light response*

Drd4-GFP mice that had received no treatment, intraocular injections of muscimol or gabazine were anesthetized with isofluorane and decapitated in accordance with the UC Berkeley Institutional Animal Care and Use Committee and conformed to the NIH Guide for the Care and Use of Laboratory Animals, the Public Health Service Policy, and the SFN Policy on the Use of Animals in Neuroscience Research. Under IR illumination, retinas were isolated from the pigment epithelium in oxygenated Ames' medium (Sigma), cut into dorsal and ventral halves, and mounted over a hole of 1–1.5 mm$^2$ on filter paper (Millipore) with the photoreceptor layer facing down. Retinas were kept in darkness at room temperature in Ames' medium bubbled with 95% O2/5% CO2 until use (0–7 hr). Recording electrodes of 3-5 Mohm were filled with Ames' medium. GFP fluorescence was detected with a custom-built, Fluoview-based two-photon microscope and a Ti:Sapphire laser (Coherent) tuned to 920nm, a wavelength that minimally activates mouse photoreceptors and therefore preserves light response. GFP cells were then targeted for loose-patch recordings using pCLAMP10 recording software and a Multiclamp 700A amplifier. Visual stimuli were generated as previously described[21]. Briefly, a white, monochromatic organic light-emitting display (OLEDXL, eMagin, Bellevue, WA, 800X 600 pixel resolution, 85 Hz refresh rate) was controlled by an Intel core duo computer with a WindowsXP OS. Drifting square-wave gratings (spatial frequency = 225 mm/cycle, temporal frequency 4 cycles/second, 30 deg/s in 12 pseudorandomly chosen directions spaced at 30 degree intervals, with each presentation lasting 3 s followed by 500 ms of gray screen) were generated from the OLED using Matlab and the Psychophysics Toolbox, and were projected through the 60x water-immersion objective (LUMPlanFl/IR, NA = 0.9) via the side port of the microscope, centered on the soma of the recorded cell, and focused on the photoreceptor layer. Loose-patch recordings were obtained during the stimulus presentation, and analyzed using Matlab. A detailed step-by-step protocol of the two-photon targeted recording of light response can be found in [27]

### *Two-photon microscopy and morphological reconstruction*

After paired recording, the Alexa 488-filled SACs and the Alexa 594-filled nDSGCs in the Drd4-GFP/mGluR2-GFP mice were imaged by the two-photon microscope at 745 nm. At this wavelength, GFP is not efficiently excited while both Alexa 488 and Alexa 594 are brightly fluorescent. Therefore, the morphology of the Alexa 488-filled SACs could be distinguished from the very weak GFP fluorescence. Image stacks were acquired at 0.5 um z-interval and resampled three times for each stack using a 60x objective (Olympus LUMPlanFl/IR 60x/0.90W), covering the entire dendritic fields of the SACs and nDSGCs. Image stacks from 25 SAC-nDSGC pairs were then imported into Neurolucida program (MBF Biosciences) and reconstructed in 3D. The density of contacts and cofasciculations (defined as the SAC and

nDSGC processes in close opposition for more than 2 um) was then quantified with the aid of NeuroExplorer software (MBF Biosciences).

### Intraocular injections

Drd4-GFP animals were anesthetized with 3.5% isoflurane/2% O2.  The eyelid was then opened with fine forceps, and 1ul of 10mM muscimol (Tocris), 500 uM gabazine (Tocris) or saline was injected using a fine glass micropipette.  Injections were made with a picospritzer (World Precision Instruments, Sarasota, FL) generating 20 psi, 3 ms long positive pressure. To prevent efflux of the injected solution, removal of the pipette tip from the eye was done slowly and gentle pressure was then applied to the injection site with a sterile cotton swab for ~10 seconds. This procedure was repeated every 48 hours, starting at P6 and ending at P12.

### Statistical analysis

Grouped data are presented as mean +/- standard deviations or standard errors as indicated. Data sets were tested for normality, and statistical differences were examined using one-way ANOVA and post hoc comparisons using Student's t-test with Bonferroni corrections(Matlab).

### Supplementary Discussion and Methods

As an independent measure of the effectiveness of muscimol at blocking retinal activity, we monitored the effect of monocular muscimol injections on the eye-specific segregation of retinogeniculate projections[3].  Though the bulk of eye-specific segregation is complete by P8, there is a small amount of additional segregation that occurs between P8 and P144, [5] To monitor the effects of activity blockade during the second postnatal week, when direction selective responses emerge, we performed intraocular injections of muscimol at P6, P8, P10 and P12, and computed the segregation index by a method that objectively quantifies the extent of segregation[2]. A significant reduction in eye-specific segregation was found in muscimol-treated animals. For a subset of experiments, eye-specific segregation was analyzed in the same brains of animals from which retinas used described in Figure 4.  However, we found no correlation between the value of the directional tuning (Figure 4) and the extent of segregation (data not shown). These findings indicate that intraocular injection of muscimol during the second postnatal week is an effective means of blocking activity in vivo.

Animals were anesthetized with 3.5% isoflurane/2% O2.  The eyelid was then opened with fine forceps to expose the eye, and 0.1-1 ul of Alexa-488 or Alexa-594 conjugated - choleratoxin was injected using a fine glass micropipette with a picospritzer (World Precision Instruments, Sarasota, FL) generating 20 psi, 3 ms long positive pressure. The cholera toxin was then allowed to transport for 24 hours, which was sufficient time for clear labeling of axons and terminals. Brains were removed, immersion fixed in 4% paraformaldehyde (24 hours), cryo-protected in 30% sucrose (18 hr) and sectioned coronally (100 μm) on a Vibratome.

Images were analyzed as described previously[2].  Briefly, eight-bit tagged image file format images were acquired for Alexa488- or 594-labeled sections of the LGN with a CCD camera (Optronics, Goleta, CA) attached to an upright microscope (Zeiss Axioscope 2; Thornwood, NY) with a 10X objective (numerical aperture, 0.45). The three sections that contained the largest ipsilateral projection, corresponding to the central third of the LGN, were selected and all analysis was performed on these sections using the side of the brain that was ipsilateral to the muscimol injection (Alexa594-labeled ipsilateral/Alexa488-labeled contralateral projection).  Background fluorescence was subtracted using a rolling ball filter (NIH Image) and

the grayscale was renormalized so that the range of grayscale values was from 0 to 256. IgorPro Software (Wavemetrics, Lake Oswego, OR) was used to perform a segregation analysis. For each pixel, we computed the logarithm of the intensity ratio, $R = \log10(FI/FC)$, where FI is the ispilateral channel fluorescence intensity and FC is the contralateral channel fluorescence intensity. We then calculated the variance of the distribution of R values for each section, which was used to compare the width of the distributions across animals. A higher variance is indicative of a wider distribution of R-values, which is in turn indicative of more contra- and ipsi- dominant pixels, and therefore more segregation.

Intraocular injection of fluorescently labeled muscimol (BODIPY TMR-X muscimol; Invitrogen) was performed according to the same protocol for unlabeled muscimol (See Methods Summary). Retinas from the injected eyes were dissected 30 min or 48 hours after injection, fixed in 4% paraformaldehyde (24 hours), and sectioned (20 μm) on a cryostat. Fluorescent images were taken with a CCD camera (Optronics).

**References:**

1. Euler, T., Detwiler, P. B. & Denk, W. Directionally selective calcium signals in dendrites of starburst amacrine cells. Nature 418, 845-52 (2002).

2. Demb, J. B. Cellular mechanisms for direction selectivity in the retina. Neuron 55, 179-86 (2007).

3. Fried, S. I., Munch, T. A. & Werblin, F. S. Mechanisms and circuitry underlying directional selectivity in the retina. Nature 420, 411-4 (2002).

4. Barlow, H. B. & Levick, W. R. The mechanism of directionally selective units in rabbit's retina. J Physiol 178, 477-504 (1965).

5. Oyster, C. W. The analysis of image motion by the rabbit retina. J Physiol 199, 613-35 (1968).

6. Ariel, M. & Daw, N. W. Pharmacological analysis of directionally sensitive rabbit retinal ganglion cells. J Physiol 324, 161-85 (1982).

7. Kittila, C. A. & Massey, S. C. Effect of ON pathway blockade on directional selectivity in the rabbit retina. J Neurophysiol 73, 703-12 (1995).

8. Weng, S., Sun, W. & He, S. Identification of ON-OFF direction-selective ganglion cells in the mouse retina. J Physiol 562, 915-23 (2005).

9. Dong, W., Sun, W., Zhang, Y., Chen, X. & He, S. Dendritic relationship between starburst amacrine cells and direction-selective ganglion cells in the rabbit retina. J Physiol 556, 11-7 (2004).

10. Famiglietti, E. V. Synaptic organization of starburst amacrine cells in rabbit retina: analysis of serial thin sections by electron microscopy and graphic reconstruction. J Comp Neurol 309, 40-70 (1991).

11. Stacy, R. C. & Wong, R. O. Developmental relationship between cholinergic amacrine cell processes and ganglion cell dendrites of the mouse retina. J Comp Neurol 456, 154-66 (2003).

12. Yoshida, K. et al. A key role of starburst amacrine cells in originating retinal directional selectivity and optokinetic eye movement. Neuron 30, 771-80 (2001).

13. Amthor, F. R., Keyser, K. T. & Dmitrieva, N. A. Effects of the destruction of starburst-cholinergic amacrine cells by the toxin AF64A on rabbit retinal directional selectivity. Vis Neurosci 19, 495-509 (2002).

14. Chen, Y. C. & Chiao, C. C. Symmetric synaptic patterns between starburst amacrine cells and direction selective ganglion cells in the rabbit retina. J Comp Neurol 508, 175-83 (2008).

15. Famiglietti, E. V. A structural basis for omnidirectional connections between starburst amacrine cells and directionally selective ganglion cells in rabbit retina, with associated bipolar cells. Vis Neurosci 19, 145-62 (2002).

16. Jeon, C. J. et al. Pattern of synaptic excitation and inhibition upon direction-selective retinal ganglion cells. J Comp Neurol 449, 195-205 (2002).

17. Jeong, S. A., Kwon, O. J., Lee, J. Y., Kim, T. J. & Jeon, C. J. Synaptic pattern of AMPA receptor subtypes upon direction-selective retinal ganglion cells. Neurosci Res 56, 427-34 (2006).

18. Chan, Y. C. & Chiao, C. C. Effect of visual experience on the maturation of ON-OFF direction selective ganglion cells in the rabbit retina. Vision Res 48, 2466-75 (2008).

19. Chen, M., Weng, S., Deng, Q., Xu, Z. & He, S. Physiological properties of direction-selective ganglion cells in early postnatal and adult mouse retina. J Physiol 587, 819-28 (2009).

20. Elstrott, J. et al. Direction selectivity in the retina is established independent of visual experience and cholinergic retinal waves. Neuron 58, 499-506 (2008).

21. Huberman, A. D. et al. Genetic identification of an On-Off direction-selective retinal ganglion cell subtype reveals a layer-specific subcortical map of posterior motion. Neuron 62, 327-34 (2009).

22. Watanabe, D. et al. Ablation of cerebellar Golgi cells disrupts synaptic integration involving GABA inhibition and NMDA receptor activation in motor coordination. Cell 95, 17-27 (1998).

23. Elstrott, J. & Feller, M. B. Direction-selective ganglion cells show symmetric participation in retinal waves during development. J Neurosci 30, 11197-201.

24. Wang, C. T. et al. GABA(A) receptor-mediated signaling alters the structure of spontaneous activity in the developing retina. J Neurosci 27, 9130-40 (2007).

25. Petreanu, L., Mao, T., Sternson, S. M. & Svoboda, K. The subcellular organization of neocortical excitatory connections. Nature 457, 1142-5 (2009).

26. Li, Y., Van Hooser, S. D., Mazurek, M., White, L. E. & Fitzpatrick, D. Experience with moving visual stimuli drives the early development of cortical direction selectivity. Nature 456, 952-6 (2008).

27. Wei, W., Elstrott, J. & Feller, M. B. Two-photon targeted recording of GFP-expressing neurons for light responses and live-cell imaging in the mouse retina. Nat Protoc 5, 1347-52.

*Supplementary References:*

1. Wang, C. T. et al. GABA(A) receptor-mediated signaling alters the structure of spontaneous activity in the developing retina. J Neurosci 27, 9130-40 (2007).

2. Torborg, C. L. & Feller, M. B. Unbiased analysis of bulk axonal segregation patterns. J Neurosci Methods 135, 17-26 (2004).

3. Huberman, A. D., Feller, M. B. & Chapman, B. Mechanisms underlying development of visual maps and receptive fields. Annu Rev Neurosci 31, 479-509 (2008).

4. Torborg, C. L. & Feller, M. B. Spontaneous patterned retinal activity and the refinement of retinal projections. Prog Neurobiol 76, 213-35 (2005).

5. Guido, W. Refinement of the retinogeniculate pathway. J Physiol 586, 4357-62 (2008).

**Figure II-1: nDSGCs receive direct GABAergic inputs from SACs located on the null and the preferred side from P4 to adult.**

a.  A fluorescence image of the ganglion cell layer from a P30 Drd4-GFP/mGluR2-GFP mouse, showing the bright membrane-bound GFP expressed under the mGluR2 promoter in the SACs and the dim cytoplasmic GFP driven by the Drd4 promoter in the nDSGC. Scale bar: 25 um.

b.  Paired whole-cell voltage-clamp recordings of GABAergic currents in a P4 nDSGC (lower traces) evoked by depolarization of a SAC from the null side (upper traces) in the presence of the NMDA receptor antagonist APV, AMPA/Kainate receptor antagonist DNQX and α4-containing nicotinic acetylcholine receptor antagonist DHBE. SACs were depolarized from -60 to 0 mV, which reliably evoked an inward current in SACs. The postsynaptic GABAergic currents were recorded in DSGC at different holding potentials to determine the current-voltage relationship of the conductance.

c.  Example images of synaptically connected, dye-filled SAC-DSGC pairs at P4, P7 and P30. The left side shows pairs with SACs (green) located on the null side of the DSGCs (red). The right side shows preferred-side pairs. Scale bar: 50 um.

d.  Soma locations of the GABAergically connected SAC-nDSGC pairs along the null-preferred axis during development. Red spots represent the positions of DSGC cell bodies. The positions of SAC cell bodies that form GABAergic synapses with their respective nDSGCs are shown as green spots; the SAC cell bodies that were not connected to nDSGCs are shown as gray spots. All pairs had overlapping dendritic fields. Scale bar: 25 um

**a**

Drd4-GFP/mGluR2-GFP

nDSGC    SAC

**b**

SAC

100 pA
5 ms

0 mV
-60 mV

DSGC

25 pA
5 ms

-10 mV
-70 mV

**c**

Null side ← Preferred side
Preferred direction

P4

P7

P30

**d**

Null side          Preferred side

P4

P7

P14-48
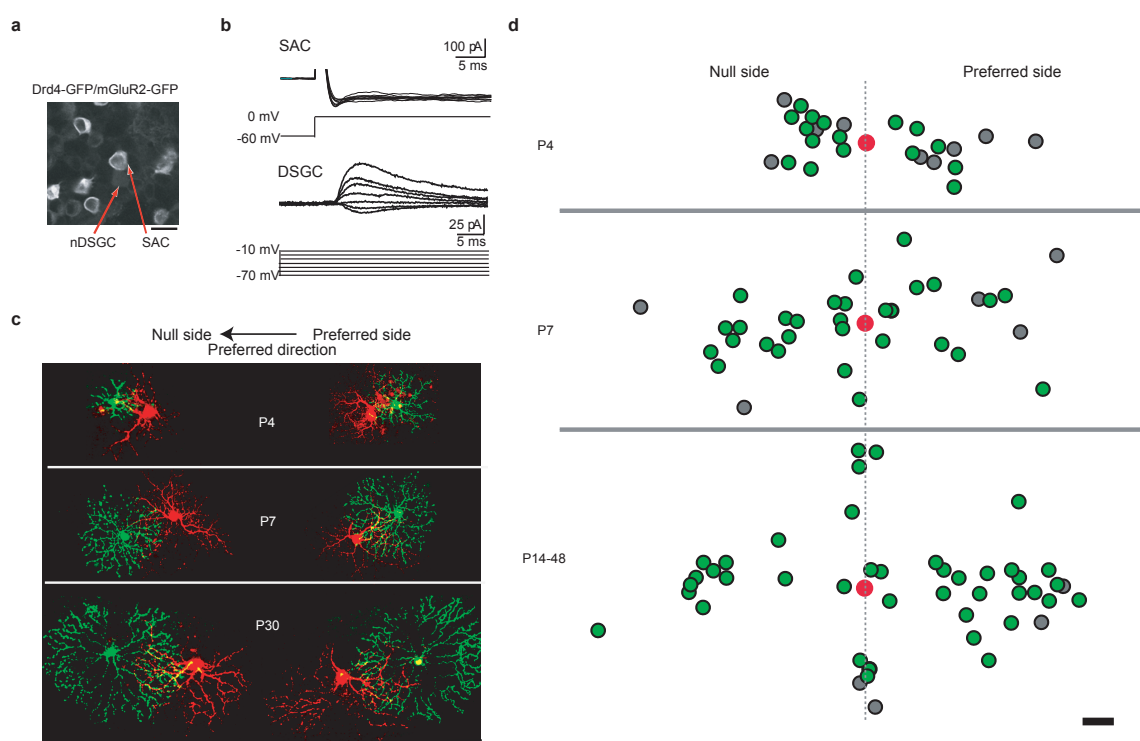
**Figure II-2: GABAergic conductance in the null-side SAC-nDSGC pairs strengthens during the second postnatal week.**

a. Postsynaptic GABAergic currents in nDSGCs recorded at holding potentials between -70 and -10 mV in response to depolarization (as in 1a) of null-side (left) and preferred-side (right) SACs at P4, P7, P14 and P30.

b. Relative soma positions of SAC-nDSGC pairs used for conductance analysis at P4, P7 and P14-48. Open circles represent nDSGC cell bodies. Filled circles are SAC somas color-coded for conductance strength normalized to the maximum value across all ages. Dashed lines illustrate average dendritic arbor diameter centered on the asterisks for nDSGCs (white) and SACs (red, asterisks represent average soma locations). Scale bar: 25 um.

c. Summary plot of GABAergic conductances of the null side and the preferred side SAC-nDSGC pairs at P4, P7 and P14-48. Individual pairs and mean values +/- standard deviations are shown. One-way ANOVA: $p < 0.0001$; t-test: *$p < 0.0001$, **$p = 0.0003$.

**a**

Null side    Preferred side

P4

100 pA
10 ms

P7

P14

P30

**b**

Null side    Preferred side

P4

P7

P14-48

0        0.5        1
Normalized conductance

**c**

P4        P7        P14-48

*

**

16

Conductance (nS)

12

8

4

0

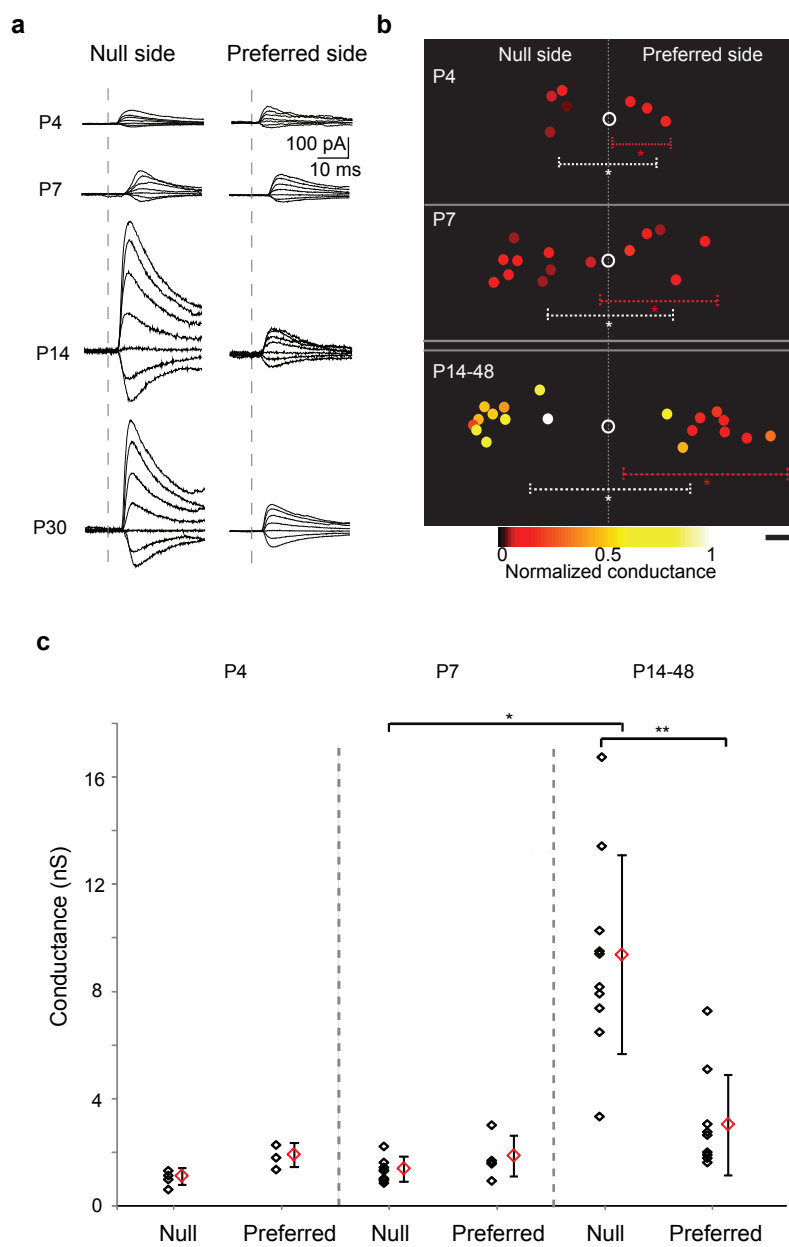Null    Preferred    Null    Preferred    Null    Preferred

**Figure II-3: Dendritic contacts and cofasciculations between SACs and nDSGCs occur at a similar density for the null and preferred side pairs.**

a. Neurolucida reconstructions of the dendrites from the On sublamina and side views of the complete dendritic arbors from a null-side (left) and a preferred-side (right) pair of SACs and nDSGCs. Dendritic contacts are shown as purple dots; cofasciculation segments are shown as white dots. Numbers (6.5 nS and 2.0 nS) are GABAergic conductance for the null-side and preferred-side pairs respectively. Scale bar: 25 um. Inset: fluorescence image of the outlined region showing dendritic contacts (arrows) and cofasciculation (arrowhead). Scale bar: 5 um.

b. Summary plot of the density of contacts between DSGCs and distal (roughly outer third of) SAC processes from the null or preferred side from P14 to 48. Individual pairs and mean values +/- standard errors are shown. The data points from $> = $ P28 are colored blue, and the ones from $<$ P28 colored black.
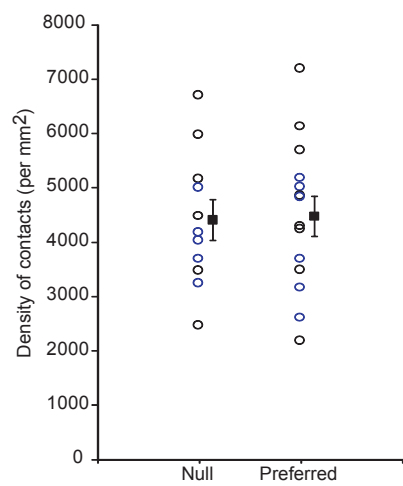
c. Summary plot of the density of cofasciculations between nDSGCs and distal SAC processes from the same pairs as in b.

Null and preferred side groups are not significantly different in b or c. $p > 0.7$, t-test.

**a**



6.5 nS

Null side ← Preferred side
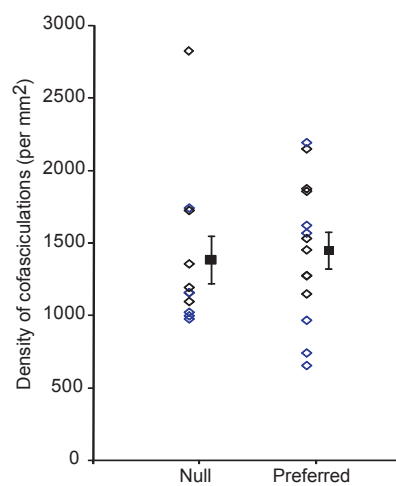Preferred direction

2.0 nS
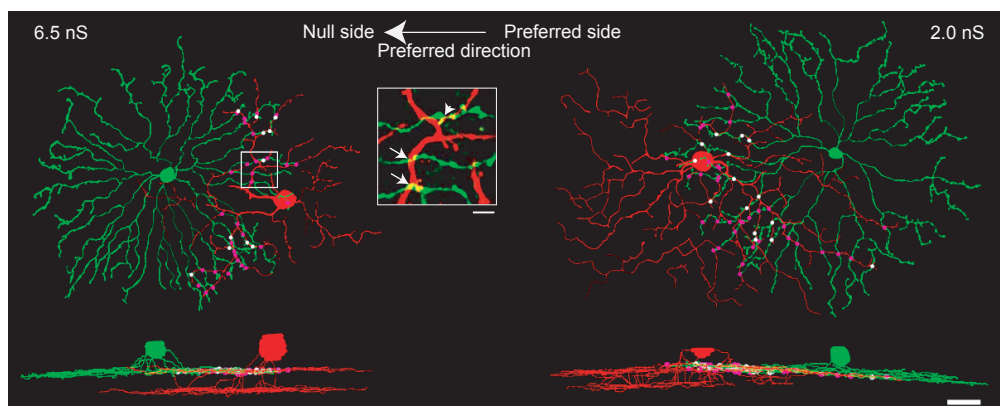
**b**



**c**

**Figure II-4: Intraocular injections of muscimol or gabazine do not alter direction selectivity in nDSGCs.**

a. The normalized spike vector sums of nDSGCs in response to drifting gratings of 12 directions from P14-15 Drd4-GFP mice that received no treatment (Control), intraocular injections of saline, muscimol, or gabazine at P6, P8, P10 and P12. N: nasal; D: dorsal; T: temporal; V: ventral. The red lines are mean vector sums of all cells in each group. Insets show examples of normalized tuning curves, with corresponding vector sums represented as red lines of nDSGCs from each group. Control: n = 4 mice, 12 cells; Saline: n = 11 mice, 43 cells; Muscimol: n = 12 mice, 25 cells; Gabazine: n = 4 mice, 17 cells.

b. Summary plot of direction selective index (DSI) for adult, P14-15 untreated, saline, muscimol and gabazine-treated groups. Bars are mean +/- standard error; open circles represent individual cells.  Adult (> P28) data are reproduced from21.

c. Example traces from whole-cell voltage-clamp recordings of inhibitory (upper traces, VH=0 mV) and excitatory (lower traces, VH=-50 mV) currents from a P14 nDSGC in drug-free ACSF (Control, left) or ACSF containing 100 µM Muscimol (right). Deflections from baseline correspond to spontaneous synaptic currents. At depolarized potentials, application of muscimol activated a tonic current, which was measured as a change in the baseline holding current[24] .

**a**

Control



Saline



Muscimol



Gabazine



**b**

DSI



**c**



Control          Muscimol

0 mV

-50 mV

100 pA
2 s
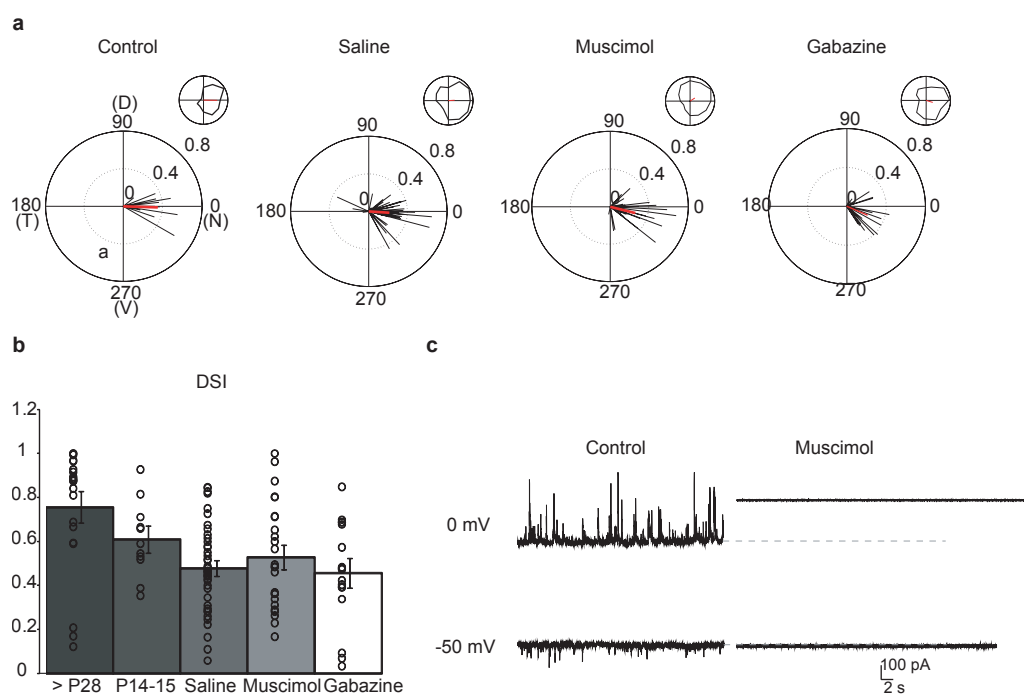
**Figure II-5. Entire processes of SACs located on the null or preferred side of DSGCs show a similar density of contacts and cofasciculations with nDSGCs dendrites.**

In Figure II-3, we restricted this analysis to the outer third of SAC processes.

a. Summary plot of the density of contacts between DSGCs and SACs from the null or preferred side from P14 to 41.

b. Summary plot of the density of cofasciculations between SACs and DSGCs from the same pairs as in a. No significant difference was found between the null and preferred side groups in a or b. $p > 0.7$, t-test.
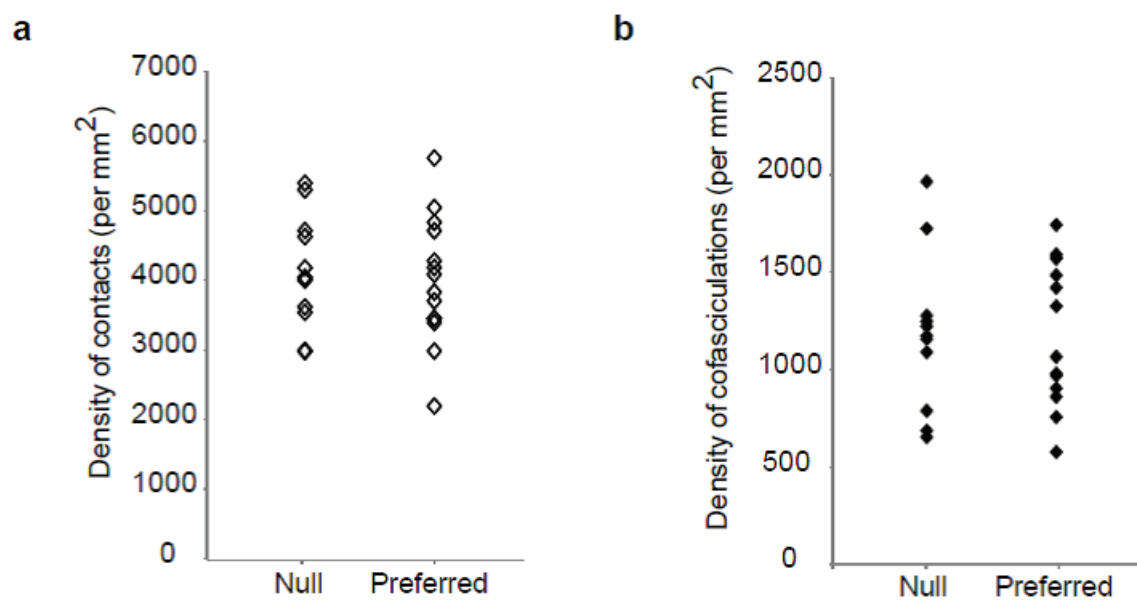
**Figure II-6: GABA-A receptor blockade abolishes direction selectivity in On-Off nDSGCs.**

a.  Light responses of a GFP+ neuron from a P14 Drd4-GFP mouse before, during and after application of the GABA-A receptor antagonist GABAzine (1.25 uM). Spike tuning curves to drifting gratings are shown in the left panel, and spike density histograms of the same cell to stationary spots in the right panel. Black bar indicates the time during which a white spot was presented.

b. Direction selective index (DSI) from five GFP+ neurons before and during GABAzine application. *p < 0.001, paired t-test
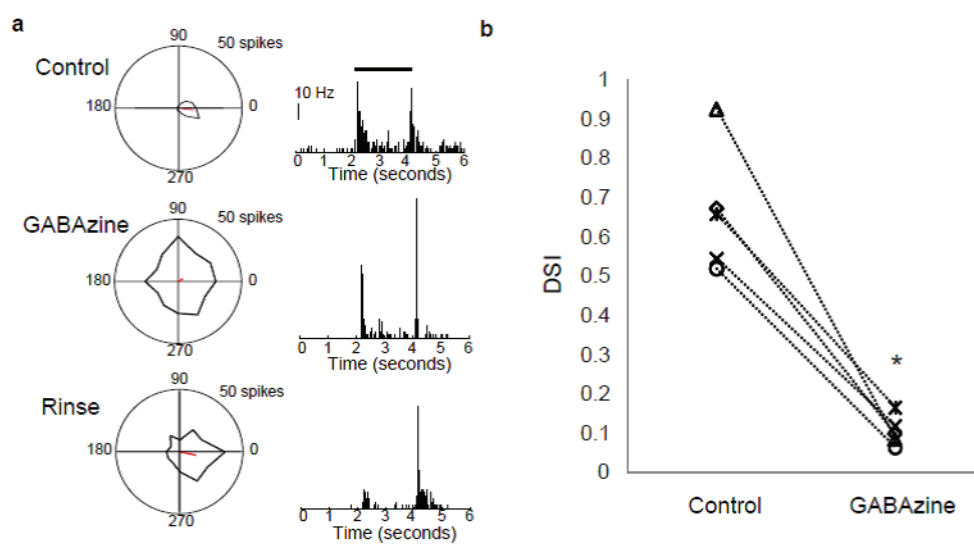
**Figure II-7: Effects of acute and chronic application of muscimol on retinal activity.**

a. Example traces from whole-cell voltage-clamp recordings of inhibitory (upper traces, VH=0 mV) and excitatory (lower traces, VH=-50 mV) currents from a P8 SAC and a P8 nDSGC in ACSF (Control, left) or ACSF containing 100 uM muscimol (right). Deflections from baseline correspond to compound synaptic currents associated with retinal waves  Note, at depolarized potentials, application of muscimol activated a tonic current, which was measured as a change in the baseline holding current1.

b. Paired whole-cell voltage-clamp recordings of inhibitory currents in a P8 nDSGC (lower traces) evoked by depolarization of a SAC from -60 mV to 0 mV (upper traces) in drug-free ACSF (Control, left) or in ACSF containing 100 uM muscimol (right).  Recording conditions were the same as in Figure 1 of the main text.

c. Fluorescence images of dorsal Lateral Geniculate Nuclei (dLGN) sections ipsilateral to the eye treated with either saline (top) or muscimol (bottom). Left, fluorescence of Alexa 594-labeled retinogeniculate axons from the treated eye; Middle, fluorescence of Alexa 488-labeled axons from the untreated eye; Right, pseudocolor images based on the logarithm of the intensity ratio, (R=log(FI/FC) ) for each pixel, a parameter that reflects the extent of segregation2.

d. Summary of the variance of the distribution of the R-values for all the pixels in the images in part a.  The broader the distribution of R-values is for a given LGN, the greater the extent of segregation (see Methods below).  Points are individual brains and error bars are standard deviation. The purple data points represent examples shown in a. *$p = 0.02$, t-test.

e. Fluorescent images of retinas from C57B/6 mice receiving no treatment (left, P6), an intraocular injection of fluorescently-labeled muscimol 30 min (middle, P6) and 48 hours (right, P8) prior to imaging. The exposure time for "No treatment" and "48 hours" was 500 ms, for "30 min" was 50 ms. Scale bar: 100 um.

a

Spontaneous activity

Control                    Muscimol

SAC    0 mV
       -50 mV

DSGC   0 mV
       -50 mV

$\llcorner$100 pA
$\llcorner$2 s

b

Evoked response

Control                    Muscimol

0 mV
-60 mV

SAC

DSGC   0 mV

200 pA
$\llcorner$60 ms

50 pA
$\llcorner$60 ms

c

Saline

Muscimol

Ipsi        Contra      log($F_I/F_C$)

1.5

-1

d

Segregation Index

Variance

0.6

0.0

*

Saline      Muscimol

e

No treatment          30 min          48 hr

OPL

IPL

GCL
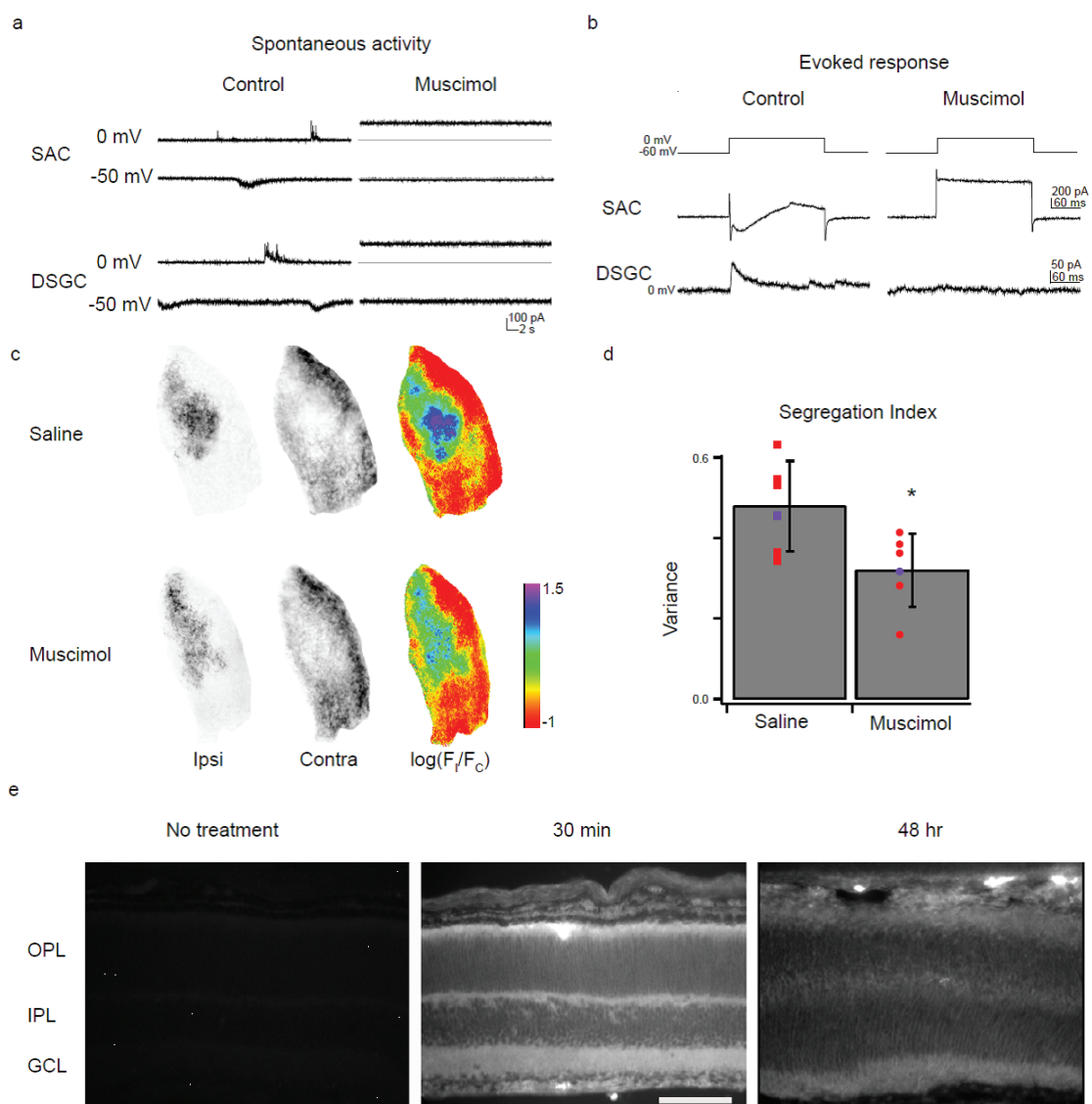
**Figure II-8: Muscimol-treated nDSGCs exhibit On and Off responses but have a higher percentage of cells that do not respond to drifting gratings.**

a and b. Summary plots of the maximum firing rate during the On (a) and Off (b) responses to stationary spots (10 repetitions, 50 ms bins) for uninjected retinas (Ctrl), retinas receiving repeated injections of saline (Sal) or muscimol (Mus). Values represent mean +/- standard deviation.

c. Summary plot of the percentage of cells not responsive to drifting gratings but exhibiting normal On-Off responses to stationary spots.

**a**

Max ON firing rate (Hz)
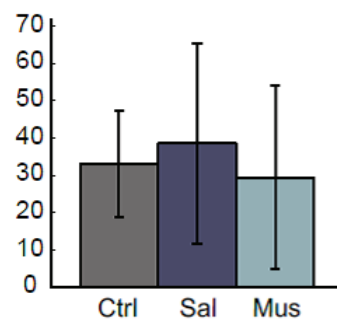


**b**

Max OFF firing rate (Hz)
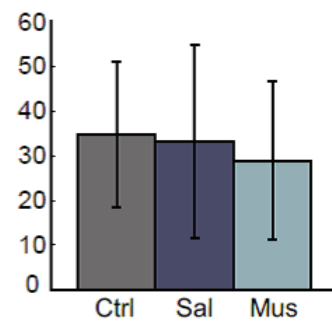


**c**

% Nonresponsive cells
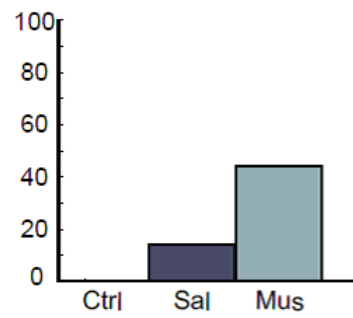
**Figure II-9: Spontaneous GABAergic IPSCs of nDSGCs show a significant increase in the frequency from P7 to P14.**

a. Whole-cell voltage-clamp recordings of spontaneous IPSCs from GFP+ neurons in P7 (top) and P14 (bottom) Drd4-GFP mice. Cells held at VH=0 mV and in the presence of 8 uM DHBE, 50 uM APV, 20 M NBQX and 1 uM TTX before (Control) and after addition of 5 uM gabazine (Gabazine).

b and c. Summary plots of the frequency (b) and peak amplitude (c) of the spontaneous IPSCs of the nDSGCs at P7 and P14. P7: n = 14 cells; P14: n = 11 cells. Error bars represent standard error. *p < 0.0001, t-test.

d. Cumulative distribution curves of the spontaneous IPSC peak amplitude for nDSGCs at P7 and P14. Shaded areas indicate standard deviation.

**a**

P7

Control

Gabazine

P14

Control

Gabazine

25 pA
100 ms

**d**

**b**

**c**
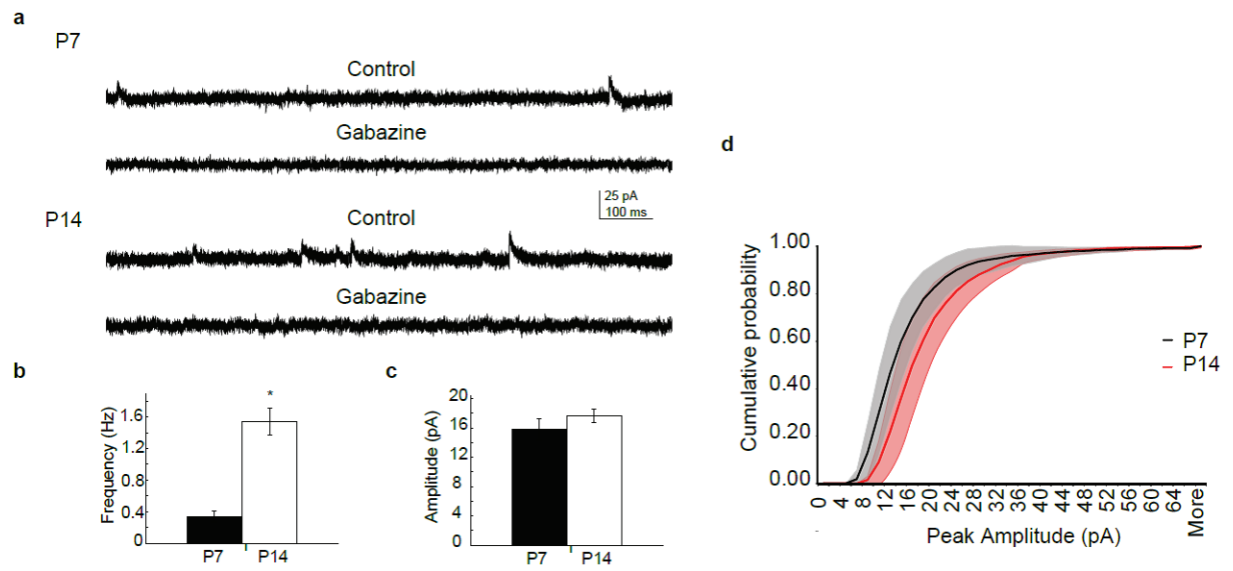
## III.   CaV 3.2 KO mice have altered retinal waves but normal direction selectivity

### Abstract

The circuit underlying retinal direction selectivity is established prior to eye opening in mice by a mechanism that involves the selective, developmental strengthening of a null-side inhibitory synapse between starburst amacrine cells (SACs) and direction-selective ganglion cells (DSGCs). During the time that direction selectivity is established, there is no vision but rather the retina spontaneously generates patterns of activity known as retinal waves. The role of retinal waves, which are characterized by periodic bursts of correlated activity, in the establishment of retinal direction selectivity is unclear. Here, using a combination of multielectrode array and cell-attached recordings we characterize the spontaneous activity and direction selectivity in a mouse lacking the CaV3.2 subunit of T-type Ca++ channels (CaV 3.2-/-). CaV3.2-/- mice exhibit altered retinal waves. Analysis of retinogeniculate projection patterns demonstrate a reduced level of eye-specific segregation in the dLGN in these mutants, indicating that the observed activity defect is sufficient to disrupt known wave-dependent developmental mechanisms. However, direction selective responses of Cav3.2-/- mice after eye-opening were indistinguishable from wild-type mice. These data indicate that bursting features of retinal waves important for activity-dependent developmental refinement of retinal projections to central targets are not critical for the development of direction selectivity.

### Introduction

A prominent feature of visual systems is that they are sensitive to motion in the visual scene. The detection of motion is first found in the retina, and this ability arises from the presence of cells that are uniquely sensitive to the direction of a moving object. One such type of cell is known as the ON / OFF direction selective retinal ganglion cell (DSGC), which consists of four subtypes, each responsive to one of the four cardinal directions of motion (nasal, temporal, dorsal ventral).

The developmental events that specify direction selective circuits in the retina are unknown. Direction selective responses are detected upon eye opening, and emerge in the absence of visual experience. Before eye opening, which occurs two weeks after birth in the mouse, the retina is not silent, but rather displays robust spontaneous activity known as retinal waves. The contribution of this spontaneous retinal activity to the development of direction selectivity is unclear; two previous manipulations, using knockout mice to significantly alter retinal waves during the first post-natal week (Elstrott et al., 2010) and chronic treatment with the silencing agent muscimol (Wei et al., 2011, Sun et al. 2011) have been unsuccessful in disrupting the development of direction selective responses, suggesting that activity is not crucial for this process. However, recent findings have identified critical developmental changes to the circuit that occur during the second post-natal week that were not likely to be affected by these previous manipulations.

One mouse line in which activity is disrupted prior to glutamatergic waves is the knockout mouse lacking the beta2 subunit of the nAChR (Bansal et al., 2000). These mice, referred to as the β2 KO mice, have dramatically altered cholinergic waves; however they were recently found to have normal direction selectivity, indicating that cholinergic waves do not contribute to the establishment of these responses (Elstrott et al., 2008). In light of the recent finding that selective synaptic strengthening underlying direction selectivity occurs in the second post-natal week (Wei et al., 2010), cholinergic waves may precede the period during which spontaneous activity is required for shaping direction selectivity and are thus not critical for its development. Rather, this period of asymmetric synaptic strengthening is coincident with glutamatergic waves, presenting the possibility that they may play a role in its development. Therefore, the goal of this study is to test the hypothesis that activity found in glutamatergic waves plays a role in the establishment of direction selective circuits in the retina.

As a first test of the role of spontaneous activity during this period, we conducted intraocular injections of the GABA-A receptor agonist muscimol, which is known to silence neuronal activity, and then recorded DS responses upon eye opening (Wei et al., 2011). Although treatment with muscimol silenced both excitatory and inhibitory postsynaptic currents in DSGCs, as well as disrupted eye-specific segregation, direction selective responses were unaffected. However, the total activity blockade provided by muscimol may have occluded a more local requirement for activity. In this case we would predict a manipulation that disrupts, but does not completely diminish, network activity to be more effective at uncovering a role for activity in the development of this circuit. Second, although treatment with muscimol disrupted eye-specific segregation, indicating an effective in vivo activity blockade, we cannot be entirely sure that activity was completely blocked throughout the entire treatment period. Third, muscimol tonically activates GABA-A receptors and may clamp starburst cell in a depolarized state, thereby leading to tonic release of transmitter. To circumvent these concerns, we sought to identify genetic models in which retinal waves are selectively altered or diminished or in which spontaneous activity is transiently blocked.

Here we describe the identification of a novel mouse model for disrupted retinal waves during the period of development when direction selectivity is established, the T-type $Ca^{2+}$ channel subunit CaV 3.2 KO (Chen et al., 2003) mouse. Voltage gated calcium channels are multi-subunit channels that activate upon membrane depolarization and allow the influx of calcium. The pore forming domain is designated as the α1 subunit, of which ten species have been identified. Each species of α1 subunit imparts a unique range of voltage sensitivity and signaling properties to the resultant channel and is a defining feature. CaV 3.2, which is the α1H subunit of the T-type Ca2+ channel (Cueni et al., 2009), is localized to bipolar cells (Pan et al., 2001), the primary source of glutamatergic inputs to retinal ganglion cells. In addition, CaV 3.2 contributes to spontaneous periodic depolarizations in bipolar cells (Ma et al., 2003). Using a multielectrode array (MEA) to compare spontaneous activity patterns in retinas from CaV3.2 KO mice and littermate controls, we find that the bursting properties of spontaneous activity patterns are dramatically altered during the second postnatal week, and that this activity perturbation leads to reduced eye-specific segregation of the retinogeniculate system. However, when both transgenically labeled posterior preferring DSGCs and whole retinal populations were assayed for direction selective responses, no difference could be detected between mice with activity

defects (KO) and those without (WT). Therefore it is unlikely that the well-timed and persistent patterns of high-frequency bursting activity seen in retinal waves play a role in the development of retinal direction selectivity.

## Results

**T-type KO mice have altered retinal waves**
In order to test the role of spontaneous activity on the development of retinal direction selective responses, we sought to identify mice with genetic deletions that produced clear and circumscribed deficits in the activity or spatiotemporal dynamics of retinal waves. Using a 60 channel multielectrode array (MEA), approximately 1 hr long recordings of spontaneous activity were made from isolated postnatal day 11-12 retinas from mice lacking the CaV3.2 isoform of T-type calcium channels and litter-mate controls and were analyzed for spiking and bursting properties as well as spatiotemporal correlation (n = 12 KO recordings, 11 WT.) (Fig 1). In Cav3.2+/+ mice, retinal waves consisted of periodic correlated bursts of action potentials, followed by an inter-wave interval that contained very few action potentials, just as we have described in wildtype mice (Blankenship et al, 2009). Cav3.2 -/- waves also contained correlated bursts of action potentials, but these bursts were separated by long periods of quiescence and the episodes of waving activity were longer than those in controls (Fig. 1A).

To quantitatively compare these firing patterns we looked at several features. First, we looked at nearest neighbor correlation as a function of distance between cells (Fig 1C). CaV3.2-/- and CaV3.2+/+ mice had similar properties, indicating that CaV3.2-/- mice exhibited propagating events. Second, non-bursting spiking properties such as mean firing rate and interspike interval were also not statistically different (mean firing rate: 0.44 Hz in KO vs. 0.69 Hz in WT. p = 0.08) between genotypes, indicating the overall amount of firing was similar.

Third, we characterized several features of the bursts, where there were pronounced differences between CaV3.2 -/- and control mice. CaV3.2 -/- retina had significantly longer burst durations and burst intervals compared to control mice (burst duration, 6 s in KO vs 1.8 s in WT; burst interval, 210 s KO vs 46s in WT). Though the burst duration was more than doubled in CaV3.2-/- compared to controls, the burst firing rate was significantly lower (7.5 Hz in KO vs. 15.8 Hz in WT). Additionally, the time spent firing above 10 hz (PC10), a feature reported to be important in driving activity-dependent effects of retinal waves such as eye-specific segregation of the dLGN (Torborg et al., 2005, Blankenship et al. 2011), was significantly reduced compared to controls (0.59% vs 1.5%).

In summary, mice lacking the CaV3.2 isoform of the T-type Ca channel exhibited propagating bursts of action potentials, but the periodicity and the properties of the spontaneous bursts were significantly altered.

We also analyzed cholinergic retinal waves in Cav3.2 -/- mice. Hence, MEA recordings were made from P6-7 retinas (n= 5 KO and 5 WT) and analyzed for the same parameters as the recordings from P11-12 mice. Though the phenotype was not as dramatic as the older mice, we found that the burst duration and burst interval were significantly altered in CaV3.2KO mice compared to controls (burst duration, 3.6s in KO vs. 2s in WT; burst interval, 106s in KO vs 54s in WT). These observations indicate that lack of CaV3.2 leads to a progressive perturbation in

the burst timing/ duration and burst firing rate of retinal waves during the second postnatal week.

Thus, the T-type KO mouse appeared to be an ideal model to test the contribution of burst properties of retinal waves on the emergence of direction selectivity.

**T-type KO mice have reduced eye-specific segregation**

To determine whether the prolonged, lower frequency bursts observed in CaV3.2 -/- mice were relevant to activity dependent processes, we assayed eye-specific segregation (ESS) of retinogeniculate projections in P16 KO and WT mice (Fig 2). Retinal waves drive the segregation of ipsi and contra retinal projections into their respective anatomical layers in the dLGN (Huberman et al., 2008; Chalupa, 2009; Feller, 2009). Manipulations that reduce correlated firing lead to deficits in the degree of segregation; therefore, we hypothesized that CaV3.2-/- mice would display reduced segregation compared to age-matched WT controls.

Retinogeniculate projections were labeled with injections of the anterograde tracer cholera-toxinB (alexa dye conjugate, 488 left eye, 568 right eye) and sections of the dLGN were prepared. By comparing the respective ipsi and contra inputs for both hemispheres of the dLGN, unbiased segregation indices were calculated to quantify the degree of segregation in KO and WT mice (Torborg and Feller, 2005). Degree of segregation is represented as the variance of the distribution of R-values for all pixels ($R=\log10 (Fi/Fc)$), with more segregated dLGNs having a wider distribution (higher variance) of R-values, compared to less segregated examples. We found that the degree of segregation for WT controls was significantly higher than in KO litter-mates (0.445 vs. 0.369, n=5 WT and 5 KO, p = 0.0079). These findings indicate that the deficits seen in the spontaneous activity patterns of CaV3.2-/- mice persist in intact animals and have an impact on ESS. They also highlight the important role of bursting properties of retinal waves, rather than spatial correlations, in driving activity-dependent developmental refinement of retinogeniculate projections.

**ON-OFF DSGCs from T-type KO mice have normal direction selective responses**

We next analyzed direction selectivity in CaV3.2-/- mice. We used two approaches. First, we crossed CaV3.2 -/- mice with a line (TRHR-GFP) that selectively labels only posterior preferring ON/OFF DSGCs (Rivlin-Etzion 2011), allowing for unambiguous targeted recordings from a known DSCG subtype. To avoid bleaching of the photoreceptors we used 2-photon targeted patch-clamp recordings and IR illumination (Huberman et al. 2009, Wei et al 2010) to identify and target DSGCs. Using the methods described in Chapter 2, we used cell-attached recordings to determine the action potential generated in response to drifting gratings to assay the degree of directional tuning. Fig 3 a and b shows a representative response from both a WT (3a) and a KO (3b) GFP(+) DSGC. All cells recorded from KO animals (n=12) displayed clear directional tuning (DSI > .4) and a clear ON/ OFF response to flashing spots, indicating that at least for TRHR-DSGCs, the emergence of mature direction selective responses are not affected by the CaV3.2-/- specific changes in spontaneous retinal activity.

In order to directly test if acute pharmacological blockade of T-type channels could affect the direction selective response, recordings were made from a TRHR(+) DSGC on a WT background in the absence and presence of up to 5um mbifradil (Fig 3C). While the magnitude of the response was reduced, the degree of tuning was unchanged, indicating that T-type channels do not play a pivotal role in the mature direction selective response. Adding additional support to this observation, all recordings to light stimuli were conducted in Ames media, which contains the known CaV3.2 specific antagonist ascorbate, at concentrations shown to inhibit channel conductance by over 75% (Nelson et al. 2007). Therefore since we are able to observe robust direction selective responses across different cell-types and recording conditions using Ames (Elstrott and Feller, 2010, Wei et al 2011) we have confidence that any potential changes to direction selective responses in the CaV3.2 -/- background are due to the circumscribed defects in spontaneous developmental activity and not as a direct consequence of CaV3.2 participation in the mature direction selective circuit.

**Large-scale MEA studies indicate that T-type KO mice have populations of DSGCs indistinguishable from WT animals**

Targeted recordings are restricted to one subtype of On-Off DSGCs (Rivlin-Etzion et al., 2011) and therefore are limited in their ability to assay generally retinal direction selectivity. Recent studies have highlighted the diverse nature of DSGC subtypes and whether specific subtypes experience differential developmental programs or influences remains unknown. To attain a more complete comparison of directional tuning between control and CaV3.2 KO mice, we used a multielectrode array. We recorded the responses of populations of RGCs from P16-19 CaV3.2-/- and control retinas in response to drifting gratings and quantified the directional selective index (DSI) of all isolated units (Fig 4) (n = 1118 WT and 1012 KO). Units having a direction selective index greater than 0.4 were considered "direction selective" (DSI > 0.4) and used for subsequent analysis of tuning width and firing rate. In order to selectively record from ON-OFF maximal velocity for ON-DSGCs but was within the tuning range for ON-OFF DSGCs (Sivyer et al., 2010).

When we compared the distribution of direction selective units, firing rates and tuning widths recorded from over 2000 units, we were unable to identify any statistically significant differences between the KO and WT populations. The distributions of DSI from WT and KO mice are almost identical (Fig 4), having an approximately normal distribution of tuning indices, with the bulk of the population centered around 0.0 (no tuning) and decreasing uniformly in frequency as tuning tended towards 1.0 (perfect tuning). Notably, many units in the CaV3.2-/- retina had high DSI's, indicating they were strongly tuned (DSI >0.8). Similarly, there appeared to be no difference between the preferred direction firing rate in control and CaV3.2 -/- RGCs. Last, we found no difference between the tuning widths of the direction selective units from KO and control retinas. Taken together, these data indicate that the altered bursting properties we observed in CaV3.2-/- mice are not critical for the development of direction selectivity in ON-OFF DSGCs.

**Discussion:**

We have identified a novel genetic model for studying the effects of altered waves on development of retinal circuits. CaV3.2 -/- mice had normal spatial correlations during waves but with altered bursting properties -- reduced periodicity, prolonged duration and lower burst firing rate. These alterations in burst properties disrupted eye-specific segregation of retinogeniculate afferents but had no effect on retinal direction selectivity. Our findings indicate that spontaneous activity during the second postnatal week, particularly during the glutamatergic regime immediately preceding eye opening does not critically contribute to the development of the direction selective responses in mice.

*CaV3.2 shapes network activity during retinal waves*
T-type channels (CaV3.1-3) differ from most other members of the voltage-gated calcium channel family (VGCC) by the range of voltages at which they are open, as well as the time for which they remain activated. Known as low-voltage activated (LVA), T-type channels are activated at lower membrane potentials than their high-voltage counterparts and inactivate quickly, giving rise to a brief transient current. This gives them the ability to generate 'pacemaker' currents and also to drive bursting activity in neurons (Perez-Reyes 2003; Cain and Snutch 2013). Although two other isoforms of T-type Ca channels exist, CaV3.2 is the overwhelmingly predominant form in DRG, where their function is well studied (Talley et al 1999; Chen et al., 2003). In the retina, numerous physiological studies indicate the presence of T-type channels in both bipolar cell terminals (Pan et al., 2001; Ma et al., 2003) and also retinal ganglion cells (Lee et al., 2003), identified by the presence of their unique T-currents. Hu et al, used electrophysiological recordings from bipolar cell slice preparations and identified what appeared to be three separate populations of bipolar cells, grouped by the T-currents they displayed, indicating that the three isoforms may be differentially expressed in subtypes of bipolar cells. Due to a lack of reliable commercially available antibodies, immunostaining data on T-type subunit expression in the retina is limited. However, a recent study from Cui et al. (2012) used a newly available antibody specific for CaV3.2 to demonstrate that this subtype is preferentially localized in the soma, dendrites, and axon terminals of type-3b cone bipolar cells. They also observed a reduction in the staining, and a loss of physiological currents, when experiments were performed in CaV3.2 -/- mice.

The changes in the firing patterns of RGCs seen in this study are likely to reflect changes in synaptic activity in the inner-plexiform layer. In particular, glutamate release from bipolar cells is likely altered by this manipulation although we cannot rule out the possibility that CaV3.2 subunit loss affects retinal excitability. Glutamate is known to be released extrasynaptically during stage III waves (Firl et al 2013) and this process, termed 'glutamate spillover' has been offered as one mechanism by which these waves propagate through the retina. How loss of CaV3.2 subunits affects glutamate release and spillover, and how those changes may relate to the altered activity seen in these mice is currently unknown. The

localization of CaV3.2 expression to non-axonal regions of bipolar cells indicate that they may underlie functions beyond regulating neurotransmitter release, such as regulation of the intrinsic excitability of bipolar cells or post-synaptic integration of synaptic input from developing photoreceptors. Direct investigation of bipolar cells from CaV3.2 deficient background by whole-cell electrophysiology or imaging will be required to acquire a better picture of how this subunit influences bipolar cell function.

The timing and frequency of action potential firing is important for synaptic plasticity and development (Zhang and Poo, 2001). Recently it was demonstrated that developing rat hippocampal GABAergic synapses exhibited long-term plasticity as a function of the frequency at which they stimulated, with low frequency stimulation leading to synaptic depression and high-frequency stimulation leading to potentiation (Xu et al. 2009). It is attractive to speculate that in the case of the developing retina, spontaneous activity may drive similar processes of activity-dependent plasticity. However, the current findings suggest that the timing and frequency of bursting activity seen in retinal waves are not critical for the observed developmental strengthening of the GABAergic synapse between the starburst amacrine cell and DSGCs.

### *Spontaneous activity is not likely to play a role in the development of retinal direction selectivity.*

Although DSGCs were first characterized over 40 years ago (Barlow et al., 1963), how the synaptic connections that specify direction selective circuits arise during development of the retina remains an outstanding question. Retinal direction selectivity appears to differ from other types of direction selective neurons in the optic tectum (Engert et al., 2002) and cortex (Li et al., 2006 and 2008) in that it is present at eye opening and does not require visual experience (reviewed in Elstrott and Feller, 2009). Since retinal direction selectivity emerges independently of visual experience, what other factors might influence the assembly of this circuit prior to eye opening? Of particular interest is the recent finding by our lab that a dramatic strengthening of the null-side inhibitory synapse between starburst amacrine cells (SAC) and DSGCs, a critical determinant in the direction selective computation, occurs between P7 and P14 (Wei et al., 2011). One possibility that has been unresolved is that spontaneous retinal activity during this period of synaptic development plays an important role in the establishment of direction selectivity.

Various properties of both spontaneous and sensory evoked neural activity have been shown to affect the development of a wide range of CNS structures and circuits (Blankenship and Feller, 2011; Zhang and Poo, 2001), including those underlying direction selective responses in V1 of ferret cortex. Numerous studies have now been conducted testing for specific roles of spontaneous and evoked activity in the development of retinal direction selectivity. As in the current study, these have included genetic approaches d(Elstrott et al. 2009) but also direct pharmacological blockade (Wei et al 2011, He 2011) and dark rearing (Elstrot. 2009). All manipulations have failed to disrupt the emergence of robust direction selectivity upon or within days of eye-opening in mice. Furthermore, the recent identification of numerous molecular 'markers' for DSGC subtypes and pre-synaptic partners, as well as the apparent genetic diversity

implied by this unexpected number of distinct DSGC subtypes indicates the likely presence of molecular cues that are involved in specifying circuit elements and partners in this system.

In a landmark study, the Fitzpatrick lab demonstrated that the receptive fields of nascent V1 pyramidal cells were poorly-tuned upon eye-opening and required sensory experience over the period of a few days to acquire their mature tuning properties. This was shown to be in contrast to the retina, where Elstrott et al. dark reared mice and found that unlike in ferret cortex, robust, near-mature direction selective responses were observable in mouse retina upon eye-opening. Thus, a model supporting a differential role for neural activity in the development of retinal and cortical direction selectivity has emerged (Elstrott and Feller, 2011). However, a recent study from Rochefort et al. (2012) has demonstrated that direction selective responses in mouse V1 are, in contrast to ferret, well-tuned upon eye-opening and insensitive to dark-rearing, complicating the simple model that retinal direction selectivity is a strictly activity-independent process, while cortical direction selectivity is strictly activity-dependent. In mouse, both the development of retinal and cortical direction selectivity appear to be relatively activity independent and very well may employ molecular, activity independent mechanisms, whereas there have been no studies in a species other than mouse that has sought to investigate the activity dependence of retinal direction selectivity. Such studies may reveal a diversity of mechanisms by which similar tuning features may emerge across species, rather than the presence of invariant developmental programs that shape similar anatomical regions across species.

In mouse there are many recent findings that, along with the inability of activity manipulations to disrupt the emergence of direction selectivity, argue for a molecularly specified circuit design. Molecular profiling to analyze various subtypes of DSGCs and also SACs (Kay et al, 2011). It was found that directional subtypes were differentially enriched with mRNA transcripts as a function of which preferred direction they would ultimately assume. Another transcript, CART (cocaine and amphetamine related transcript) was also uniquely expressed by only bistratified (ON-OFF) DSGCs and SACs. Thus it appears as though a rudimentary molecular code may exist to specify subtype choice and to promote association with SACs, a pivotal pre-synaptic partner. Future experiments are needed to further elucidate this process and provide a more detailed account of the molecular basis of subtype choice, but also of the synaptic contacts made between SACs, bipolar cells and DSGCs and their selective strengthening or weakening.

While it does not seem likely that spontaneous activity plays a role in the development of direction selectivity in the retina, there may still be a more general role for visually evoked activity in the maturation of the distinct cardinal grouping of DSGC subtypes in the mature retina. Chan and Chao (2013) showed that upon eye-opening in rabbit and mouse the distribution of preferred directions was uniformly distributed, rather than showing segregation along the four cardinal axes, indicating that a process of refinement in the preferred direction occurs after eye-opening.  also found a slight degree of anisotropy in the distribution of preferred directions in dark reared animals. These findings suggest that the process of establishing strong null-side inhibition that underlies direction selectivity may differ from the mechanism that ultimately determines functional preferred direction in DSGCs and that activity may play a role in the latter.

This study demonstrates that the CaV3.2 subunit of the T-type Ca channel is important for shaping bursting activity that occurs during retinal waves. Its absence likely affects release from bipolar cells and converts brief, regular bouts of high-frequency bursting into longer, less frequent low-frequency episodes. Although the circuit that underlies direction selectivity coincidently undergoes a period of critical synaptic maturation during this time, introducing a persistent and dramatic alteration in the activity present during the second postnatal week did not affect the development of robust directional responses after eye-opening. These results and others indicate that the final stages of development in the direction selective circuit in the retina do not require spontaneous activity.

## Methods

### *Mice:*
P11-19 CaV3.2 -/- mice and litter-mate controls were maintained on a C57bl/6 background and housed under constant day/night cycles and provided food and water ad libidum.

### *Multi-electrode array recordings of spontaneous activity*:
Retinas were removed from CaV3.2 KO and WT mice at P11-12 in room light and perfused with oxygenated and pH buffered ACSF and placed ganglion cell side down on a commercial 61 electrode array. Approximately 1 hour recordings of spontaneous activity were made and analyzed as described below.

### *Multi-electrode array recordings of visual responses:*
Retinas were removed from CaV3.2 KO and WT mice at P16 in the dark under infra-red illumination and placed ganglion cell side down on a commercial 61 electrode array. The presence or absence of direction selective responses was then characterized by stimulating the retina with square pulse drifting gratings presented on a small LED display placed in the camera port of the microscope. The photoreceptor layer of the isolated piece of retina will be stimulated from above with an optically reduced image of a CRT monitor focused with a microscope objective, centered on the array, and refreshing at 120 Hz (gray screen intensity = 1623.491 nm equivalent photons/$\mu m2/s$). For most experiments, the retina was stimulated with five repetitions of full-field square wave gratings moving in one of 12 randomly interleaved directions, with each presentation lasting 10 s, followed by 3 s of gray screen (800 $\mu m$/period, 1.066 s/period, velocity = 25 deg/s for the adult mouse; (Remtulla and Hallett, 1985). In some recordings, full-field sinusoidal gratings may be used (400 $\mu m$/period, 0.533 s/period, velocity = 25 deg/s for the adult mouse).

### *Spike-sorting:*
The voltage trace recorded on each electrode were sampled at 20 kHz and stored for offline analysis. Spikes that cross threshold were sorted according to the principal components of their voltage waveforms on neighboring electrodes. Spikes were first projected into the first five principal component dimensions where an expectation maximization algorithm was used to group spikes into a mixture of Gaussians model. All spike clusters will be inspected manually in principal component space.  The overall direction selective response was characterized in each direction by computing the vector sum of these responses for each cell. A direction selective

index is then calculated for each cell, given by the following formula: D.I.= ( pref - null)/( pref + null) where pref is the average response in the preferred direction, defined as the stimulus direction closest to the vector sum of all responses, and null is the average response in the stimulus direction 180 degrees opposite pref. For a given cell, the maximum  The width of the tuning curve, which is a measure of the strength of directional tuning and defines the preferred and null axis for each DSGC, is computed by fitting the response curve to a von-Mises distribution, given by the following: R = Rmaxek cos(x−μ) /ek where R is the response to motion in a given stimulus direction x in radians, Rmax is the maximum response, μ is the preferred direction in radians, and k is the concentration parameter accounting for tuning width. The tuning width of each cell will be estimated as the full width at half height (fwhh) of the von Mises fit using the following equation: fwhh = 2(θ − μ), where θ = acos [ln( ½ ek + ½  e- k)/ k] + μ. Calculating these values allows us to investigate the degree of tuning in nascent DSGCs that have experienced altered activity. Mean firing rates in the preferred and null directions were computed as previously described (Elstrott et al., 2008).

*Eye-specific segregation analysis:*
Animals were anesthetized with 3.5% isoflurane/2% O2.  The eyelid was then opened with fine forceps to expose the eye, and 0.1-1 ul of Alexa-488 or Alexa-594 conjugated-choleratoxin was injected using a fine glass micropipette with a picospritzer (World Precision Instruments, Sarasota, FL) generating 20 psi, 3 ms long positive pressure. The cholera toxin was then allowed to transport for 24 hours, which was sufficient time for clear labeling of axons and terminals. Brains were removed, immersion fixed in 4% paraformaldehyde (24 hours), cryo-protected in 30% sucrose (18 hr) and sectioned coronally (100 μm) on a Vibratome.

Images were analyzed as described previously. Eight-bit tagged image file format images were acquired for Alexa488- or 594-labeled sections of the LGN with a CCD camera (Optronics, Goleta, CA) attached to an upright microscope (Zeiss Axioscope 2; Thornwood, NY) with a 10X objective (numerical aperture, 0.45). The three sections that contained the largest ipsilateral projection, corresponding to the central third of the LGN, were selected and all analysis was performed on these sections using the side of the brain that was ipsilateral to the muscimol injection (Alexa594-labeled ipsilateral/Alexa488-labeled contralateral projection).  Background fluorescence was subtracted using a rolling ball filter (NIH Image) and the grayscale was renormalized so that the range of grayscale values was from 0 to 256. IgorPro Software (Wavemetrics, Lake Oswego, OR) was used to perform a segregation analysis. For each pixel, we computed the logarithm of the intensity ratio, R=log10(FI/FC), where FI is the ispilateral channel fluorescence intensity and FC is the contralateral channel fluorescence intensity. We then calculated the variance of the distribution of R values for each section, which was used to compare the width of the distributions across animals.  A higher variance is indicative of a wider distribution of R-values, which is in turn indicative of more contra- and ipsi- dominant pixels, and therefore more segregation

# References

Allen TA, Narayanan NS, Kholodar-Smith DB, Zhao Y, Laubach M, Brown TH. (2008) Imaging the spread of reversible brain inactivations using fluorescent muscimol.J Neurosci Methods. 2008 Jun 15;171(1):30-8. Epub Mar 10.

Amthor FR, Oyster CW (1995): Spatial organization of retinal information about the direction of image motion. Proc Natl Acad Sci U S A 92:4002-4005.

Bansal A, Singer JH, Hwang BJ, Xu W, Beaudet A, Feller MB. (2000) Mice lacking specific nicotinic acetylcholine receptor subunits exhibit dramatically altered spontaneous activity patterns and reveal a limited role for retinal waves in  forming ON and OFF circuits in the inner retina. J Neurosci. 2000 Oct15;20(20):7672-81.

Barlow HB, Hill RM (1963): Selective sensitivity to direction of movement in ganglion cells of the rabbit retina. Science, 139:412-414.

Blankenship AG and Feller MB (2009): Spontaneous Activity in the Developing Nervous System Nature Neuroscience Reviews

Cain SM, Snutch TP (2013) T-type calcium channels in burst-firing, network synchrony, and epilepsy. Biochim Biophys Acta. 2013 Jul;1828(7):1572-8

Chan YC, Chiao CC (2008). Effect of visual experience on the maturation of ON-OFF direction selective ganglion cells in the rabbit retina. Vision Res. Oct; 48(23-24):2466-75

Chan YC, Chiao CC (2013) The distribution of the preferred directions of the ON-OFF direction selective ganglion cells in the rabbit retina requires refinement after eye opening.  Physiol Rep. 2013 Jul;1(2)

Chen CC, Lamping KG, Nuno DW, Barresi R, Prouty SJ, Lavoie JL, Cribbs LL, England SK, Sigmund CD, Weiss RM, Williamson RA, Hill JA, Campbell KP (2003)    Science. 2003 Nov 21;302(5649):1416-8.

Chen M, Weng S, Deng Q, Xu Z, He S (2009) Physiological properties of  directionselective ganglion cells in early postnatal and adult mouse retina. J    Physiol. Feb 15;587(Pt 4):819-28.

Demb JB (2007) Cellular mechanisms for direction selectivity in the retina. Neuron. Jul 19;55(2):179-86.

Elstrott J, Anishchenko A, Greschner M, Sher A, Litke AM, Chichilnisky EJ, Feller MB  (2008): Direction selectivity in the retina is established independent of visual experience and cholinergic retinal waves. Neuron, 58:499-506.

Elstrott J, Feller MB (2009) Vision and the establishment of direction-selectivity: a tale of two circuits. Curr Opin Neurobiol. Jun;19(3):293-7.

Engert F, Tao HW, Zhang LI, Poo MM (2002): Moving visual stimuli rapidly induce Direction sensitivity of developing tectal neurons. Nature, 419:470-475.

Fried SI, Munch TA, Werblin FS (2002): Mechanisms and circuitry underlying directional selectivity in the retina. Nature, 420:411-414.

Fried SI, Masland RH (2007) Image processing: how the retina detects the direction of image motion. Curr Biol. Jan 23;17(2):R63-6.

Guido W. (2008) Refinement of the retinogeniculate pathway. J Physiol. Sep 15;586(Pt 18):4357-62.

Huang ZJ (2009) Activity-dependent development of inhibitory synapses and innervation pattern: role of GABA signalling and beyond. J Physiol. 2009 May 1;587(Pt9):1881-8.

Huberman AD, Wei W, Elstrott J, Stafford BK, Feller MB, Barres BA (2009) Genetic identification of an On-Off direction-selective retinal ganglion cell subtype reveals a layer-specific subcortical map of posterior motion. Neuron. May 14;62(3):327    34.

Huberman AD, Feller MB, Chapman B (2008) Mechanisms underlying development of visual maps and receptive fields. Annu Rev Neurosci 31:479-509

Kerschensteiner D, Morgan JL, Parker ED, Lewis RM, Wong RO (2009).  Neurotransmission selectively regulates synapse formation in parallel circuits in vivo. Nature Aug 20;460(7258):1016-2

Kim IJ, Zhang Y, Yamagata M, Meister M, Sanes JR (2008) Molecular identification of a retinal cell type that responds to upward motion. Nature, 452:478-482.

Lee SC, Hayashida Y, Ishida AT (2003) Availability of low-threshold $Ca^{2+}$ current in retinal ganglion cells. J Neurophysiol. 2003 Dec;90(6):3888-901.

Li Y, Van Hooser SD, Mazurek M, White LE, Fitzpatrick D (2008). Experience with moving visual stimuli drives the early development of cortical direction selectivity. Nature. Dec 18;456(7224):952-6.

Ma YP, Pan ZH (2003) Spontaneous regenerative activity in mammalian retinal bipolar   cells: roles of multiple subtypes of voltage-dependent Ca2+ channels Vis Neurosci. 2003 Mar-Apr;20(2):131-9

Martin JH, Ghez C (1999) Pharmacological inactivation in the analysis of the central control of movement. J Neurosci Methods. Jan;86(2):145-59

McLaughlin T, Torborg CL, Feller MB, O'Leary DD (2003) Retinotopic map refinement requires spontaneous retinal waves during a brief critical period of development. Neuron, 40:1147-1160.

Nakashiba T, Young JZ, McHugh TJ, Buhl DL, Tonegawa S (2008). Transgenic   inhibition of synaptic transmission reveals role of CA3 output in hippocampal    learning. Science. Feb 29;319(5867):1260-4.

Oyster CW, Barlow HB (1967): Direction-selective units in rabbit retina: distribution of preferred directions. Science, 155:841-842.

Pan ZH, Hu HJ, Perring P, Andrade R (2001): T-type Ca(2+) channels mediate neurotransmitter release in retinal bipolar cells. Neuron. 2001 Oct 11;32(1):89-98

Sernagor E, Eglen SJ, Wong RO (2001): Development of retinal ganglion cell structure and function. Prog Retin Eye Res 2001, 20:139-174.

Stewart DL, Chow KL, Masland RH (1971) Receptive-field characteristics of lateral geniculate neurons in the rabbit. J Neurophysiol 1971, 34:139-147.

Sun LO, Jiang Z, Rivlin-Etzion M, Hand R, Brady CM, Matsuoka RL, Yau KW, Feller MB, Kolodkin AL (2013) On and off retinal circuit assembly by divergent molecular mechanisms. Science. 2013 Nov 1;342(6158)

Taylor WR, Vaney DI (2002) Diverse synaptic mechanisms generate direction selectivity in the rabbit retina. J Neurosci 2002, 22:7712-7720.

Torborg CL, Feller MB (2004): Unbiased Analysis of Bulk Axonal Segregation Patterns. Journal of Neuroscience Methods 2004, 135

Torborg CL, Hansen KA, Feller MB (2005): High frequency, synchronized bursting drives eye-specific segregation of retinogeniculate projections. Nat Neurosci 2005, 8:72- 78.

Vaney DI, Peichl L, Wassle H, Illing RB (1981) Almost all ganglion cells in the rabbit retina project to the superior colliculus. Brain Res 1981, 212:447-453.

Wang C-T, Blankenship A, Anishchenko A, Elstrott J, Fikhman M, Nakanishi S, Feller M:GABA-A receptor-mediated signaling alters the structure of spontaneous activity in the developing retina. Journal of neuroscience 2007

Wei W, Hamby AM, Zhou K, Feller MB: Development of asymmetric inhibition underlying direction selectivity in the retina. Nature, 2011

Wong RO, Ghosh A (2002) Activity-dependent regulation of dendritic growth and patterning. Nat Rev Neurosci. Oct;3(10):803-12.

Xu C, Zhao MX, Poo MM, Zhang XH. GABA(B) receptor activation mediates frequency dependent plasticity of developing GABAergic synapses. Nat Neurosci. 2008 Dec;11(12):1410-8

Xu HP, Chen H, Ding Q, Xie ZH, Chen L, Diao L, Wang P, Gan L, Crair MC, Tian N. The immune protein CD3zeta is required for normal development of neural circuits in the retina. Neuron. 2010 Feb 25;65(4):503-15.

Yoshida K, Watanabe D, Ishikane H, Tachibana M, Pastan I, Nakanishi S: A key role of starburst amacrine cells in originating retinal directional selectivity and optokinetic eye movement. Neuron 2001, 30:771-780.

Zhang LI, Poo MM (2001) Electrical activity and development of neural circuits Nat
	Neurosci. Nov;4 Suppl:1207-14

**Figure III-1:   CaV 3.2 -/- mice have altered retinal waves**

A.  Spike rasters from hour long MEA recordings of P11 Wt and KO retinas. Bottom panels show average firing rate.

B. Wave statistics from MEA recordings of P11 Wt and KO retinas Wt n=12; KO n= 11) . Significant difference was considered to be $p < 0.05$.

C. Summary plots of wave statistics and nearest neighbor correlation index for all MEA recordings (Wt n=12; KO n= 11)
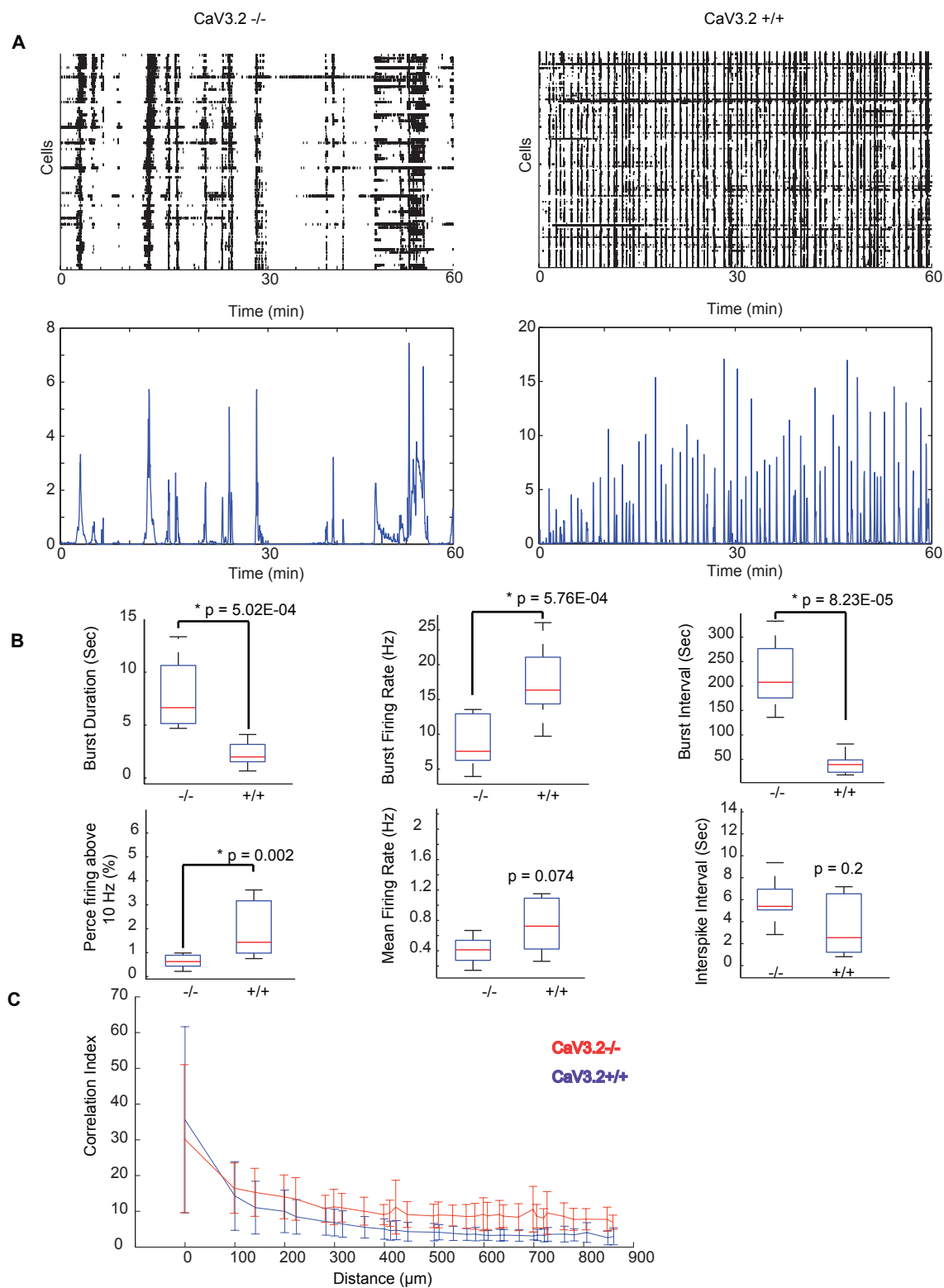
**A**

CaV3.2 -/-

CaV3.2 +/+

**B**

**C**

CaV3.2-/-
CaV3.2+/+

**Figure III-2:  CaV3.2 -/- mice have reduced eye-specific segregation**

A. Images of P16 KO and WT dorsal lateral geniclate nuclei (dLGN) sections labeled with Cholera toxin B (CTB)

B. Summary of the variance of the distribution of the R values for all the pixels in the images in part A.
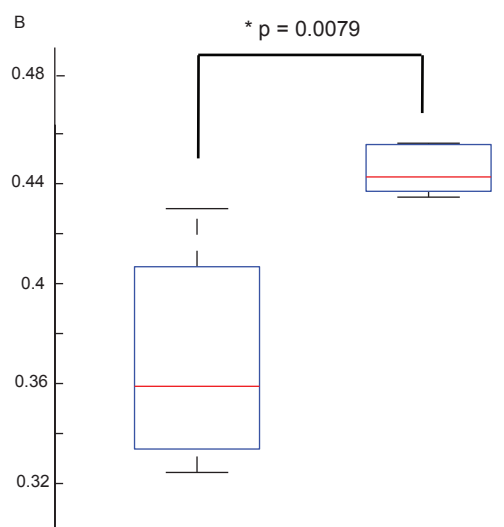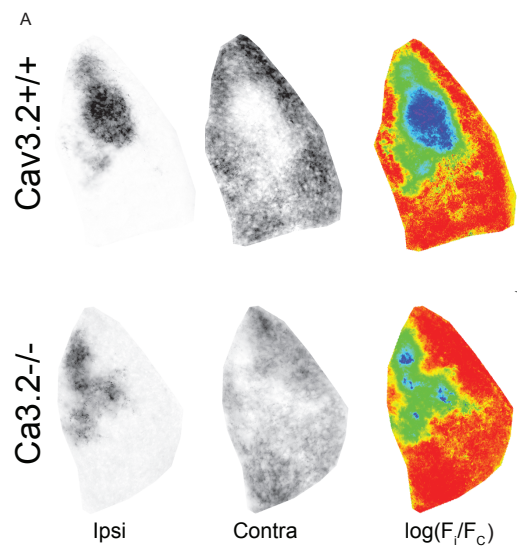
A

Cav3.2+/+

Ca3.2-/-

Ipsi          Contra          $\log(F_i/F_C)$

B

* p = 0.0079

**Figure III-3: On-OFF DSGCs from CaV3.2 -/- mice have normal direction selective responses**

A and B. Targeted 2-photon recordings of light responses from GFP(+) cells in WT(A) and KO (B) P18 TRHR mice.

C. Targeted 2-photon recordings of light responses from GFP(+) cells in a P23 TRHR mouse, before, during and after bath application of the T-type channel blocker, mbifradil (5uM). Results indicate that blocking T-type channels does not significantly alter direction selectivity (DSI pre: 0.78; DSI drug: .47), indicating that in adult retina, T-type channels do not contribute signifcantly to the direction selective circuit.
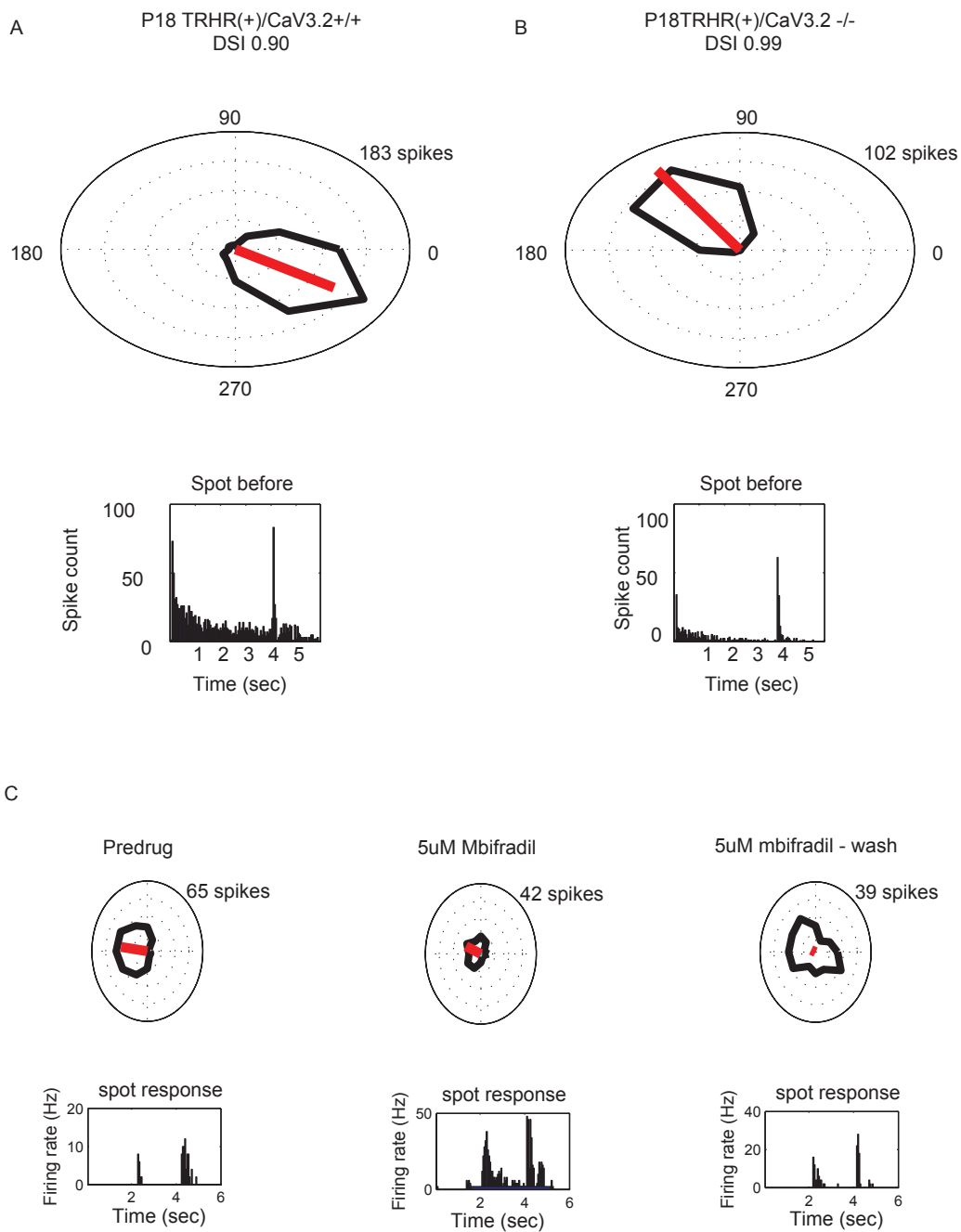
A

P18 TRHR(+)/CaV3.2+/+
DSI 0.90



B

P18TRHR(+)/CaV3.2 -/-
DSI 0.99



C

Predrug

5uM Mbifradil

5uM mbifradil - wash

**Fig III-4:  Populations of RGCs from CaV3.2 -/- mice have directional responses indistinguishable from WT**

A. Example direction selective units recorded on a multi-electrode array from WT and KO P18 mice. Well-tuned units are present in both genotypes.

B. Summary data for direction selectivity index (DSI) from all WT and KO units (n= 1118 WT, 1012 KO).

C and D. Summary data for all units with DSI > 0.4 from WT and KO units; Maximum firing rate in the preferred direction is shown in C; Distribution of tuning widths is shown in D. Data indicate that direction selective responses from WT and KO populations are identical.